



# Influence of cyclonic and anticyclonic eddies on plankton in the southeastern Mediterranean Sea during late summertime

Natalia Belkin<sup>1</sup>, Tamar Guy-Haim<sup>1</sup>, Maxim Rubin-Blum<sup>1</sup>, Ayah Lazar<sup>1</sup>, Guy Sisma-Ventura<sup>1</sup>, Rainer Kiko<sup>2</sup>, Arseniy R. Morov<sup>1</sup>, Tal Ozer<sup>1</sup>, Isaac Gertman<sup>1</sup>, Barak Herut<sup>1</sup>, and Eyal Rahav<sup>1</sup>

<sup>1</sup>Israel Oceanographic and Limnological Research, Haifa, Israel

<sup>2</sup>Sorbonne Université, Laboratoire d’Océanographie de Villefranche, Villefranche-sur-Mer, France

**Correspondence:** Eyal Rahav (eyal.rahav@ocean.org.il) and Natalia Belkin (belkin@ocean.org.il)

Received: 26 December 2021 – Discussion started: 6 January 2022

Revised: 10 March 2022 – Accepted: 11 April 2022 – Published: 13 May 2022

**Abstract.** Planktonic food webs were studied contemporaneously in a mesoscale cyclonic (upwelling, ~13 months old) and an anticyclonic (downwelling, ~2 months old) eddy as well as in an uninfluenced background situation in the oligotrophic southeastern Mediterranean Sea (SEMS) during late summer 2018. We show that integrated nutrient concentrations were higher in the cyclone compared to the anticyclone or the background stations by 2–13-fold. Concurrently, *Synechococcus* and *Prochlorococcus* were the dominant autotrophs abundance-wise in the oligotrophic anticyclone (~300 × 10<sup>10</sup> cells m<sup>-2</sup>). In the cyclone, functional groups such as dinoflagellates, Prymnesiophyceae and Ochrophyta contributed substantially to the total phytoplankton abundance (~14 × 10<sup>10</sup> cells m<sup>-2</sup>), which was ~65 % lower at the anticyclone and background stations (~5 × 10<sup>10</sup> cells m<sup>-2</sup>). Primary production was highest in the cyclonic eddy (191 mg C m<sup>-2</sup> d<sup>-1</sup>) and 2–5-fold lower outside the eddy area. Heterotrophic prokaryotic cell-specific activity was highest in the cyclone (~10 fg C cell<sup>-1</sup> d<sup>-1</sup>), while the least productive cells were found in the anticyclone (4 fg C cell<sup>-1</sup> d<sup>-1</sup>). Total zooplankton biomass in the upper 300 m was 10-fold higher in the cyclone compared with the anticyclone or background stations (1337 vs. 112–133 mg C m<sup>-2</sup>, respectively). Copepod diversity was much higher in the cyclone (44 species), compared to the anticyclone (6 small-size species). Our results highlight that cyclonic and anticyclonic eddies show significantly different community structure and food-web dynamics in oligotrophic environments, with cyclones representing productive oases in the marine desert of the SEMS.

## 1 Introduction

The southeastern Mediterranean Sea (SEMS) is an ultra-oligotrophic marine system (Berman et al., 1984) with low and patchy standing stocks of phytoplankton (Christaki, 2001; Efrati et al., 2013) and zooplankton (Pasternak et al., 2005; Siokou-Frangou et al., 2002). Phytoplankton are bottom-up controlled by N and P (Tanaka et al., 2011; Zohary et al., 2005) and heterotrophic bacteria are limited by P (Sala et al., 2002; Thingstad et al., 2005; Zohary and Robarts, 1998), dissolved organic P (DOP, Van Wambeke et al., 2002; Djaoudi et al., 2018; Sisma-Ventura and Rahav 2019) and/or dissolved organic C (DOC, Hazan et al., 2018; Rahav et al., 2019). The phytoplankton community is mostly comprised of cyanobacteria and pico-sized microbial eukaryotes with a high surface-area-to-volume ratio (Berman-Frank and Rahav, 2012; Ignatiades et al., 2002) that enables a faster nutrient uptake from the environment (Campbell and Vaulot, 1993). The low phytoplankton standing stocks lead to low primary production rates of 32–60 g C m<sup>-2</sup> yr<sup>-1</sup> (López-Sandoval et al., 2011; Psarra et al., 2000). Zooplankton biomass is usually coupled with that of the phytoplankton and is mostly comprised of mesozooplankton that feed on pico-phytoplankton (Dolan and Marrasé, 1995; Pitta et al., 2001) or other mesozooplankton (Christou, 1998; Pasternak et al., 2005).

Alterations in plankton biomass or activity from their typically low values can be found episodically in the SEMS at distinct hydrologic discontinuities such as cyclonic (upwelling) and anticyclonic (downwelling) eddies (Christaki et al., 2011; Groom et al., 2005; Rahav et al., 2013). These

geostrophically balanced mesoscale structures can span tens to hundreds of kilometers in diameter (Groom et al., 2005; Robinson and Golnaraghi, 1994). These high-energy eddies may retain plankton communities over timescales of weeks to months (Christaki et al., 2011; Menna et al., 2012; Rahav et al., 2013) and affect limiting nutrient levels at the euphotic zone (Condie and Condie, 2016). Therefore, the transport of potential and kinetic energy, nutrients, and biota by eddies (cyclonic or anticyclonic) may alter phytoplankton and zooplankton biomass and activity (Allen et al., 1996; Falkowski et al., 1991).

In this study, we report the results of physical, chemical and biological samplings of two contrasting sites in the SEMS deep waters: cyclonic and anticyclonic eddies as well as a background, uninfluenced station. We sampled these stations at the end of summer when the most oligotrophic conditions prevail in the photic layer (Kress et al., 2014; Rahav et al., 2019). We hypothesized that the upward advection of deep and relatively cold nutrient-rich water within the cyclonic eddy enhances primary production as well as the biomass of pico-eukaryotes and zooplankton. By contrast, downwelling circulation at the anticyclonic eddy yields ultra-oligotrophic conditions, even more than those of the background waters of the SEMS, leading to low phytoplankton biomass and production, the predominance of cyanobacteria, and low zooplankton biomass.

## 2 Methods

### 2.1 Study area and seawater collection

Water samples were collected during 9–11 October 2018 on board the R/V *Bat-Galim* in three distinct water habitats: (1) the core of an anticyclonic eddy (32.14° N, 33.59° E), (2) the core of a cyclonic eddy (33.16° N, 33.86° E), and (3) a station uninfluenced by eddy circulation (hereafter referred to as “background”; 32.95° N, 34.46° E) (Fig. 1a). The eddy’s core locations were determined a few days prior to the cruise and were updated until the morning of the cruise by maps created with the Angular Momentum Eddy Detection and tracking Algorithm (AMEDA) (Le Vu et al., 2018) applied to AVISO/CMEMS sea surface height (SSH) data, which were produced especially for this mission. This algorithm tracks individual eddies and accounts for successive merging and splitting incidents between eddies. It also corrects for cyclostrophic balance of the surface velocity field, which allows for a better representation of intense eddies (Ioannou et al., 2019). A more detailed characterization of the physical structure of the water column inside or outside the different cores was collected during the cruise and a few days afterward using a SeaExplorer glider equipped with temperature and salinity sensors (see below). The cruise was part of a cooperation with the Pelagic Ecosystem Response to dense water formation in the Levant (PERLE) cam-

paign, which is one of the three operations of the MER-MEX (Marine Ecosystem Response in the Mediterranean EXperiment, <https://mermex.mio.univ-amu.fr/>, last access: May 2022) project. As such, it coincided with the project’s standard sampling protocols.

Seawater was sampled using Niskin bottles (8 L each) mounted on a rosette equipped with a temperature, conductivity, depth sensor (CTD) (Seabird 9 Plus) and a fluorometer (Sea-Point). Five to six water depths were sampled at each station which represented the main oceanographic features within the water column derived from real-time CTD and fluorometer data: the surface (2 m), the bottom of the mixed layer depth (30–60 m), the deep chlorophyll *a* area (60–165 m) and the bottom of the photic layer (180 m). An additional offshore station uninfluenced by eddy circulation (station THMO1) was sampled in a parallel cruise at the SEMS on the same date as our study in greater detail (11 depths within the photic layer, Reich et al., 2022). The chemical and chlorophyll *a* profiles were not significantly different between the THMO1 and our background stations (Kruskal–Wallis one-way analysis of variance on ranks,  $P > 0.05$ , Fig. S1 in the Supplement), thus giving credibility to our measurements which comprised only five to six depths in the photic layer. Mesozooplankton were sampled using vertical WP2 hauls ( $\varnothing$  57 cm, 50  $\mu$ m mesh size, Hydro-Bios, Germany) hoisted at 0.5  $\text{m s}^{-1}$  from 300 m to the water surface during nighttime (19:00–06:00). The southeastern Mediterranean Sea is an extremely oligotrophic region, with very low zooplankton densities, especially in the large-size fraction (Koppellmann et al., 2009). It was therefore stressed that the standard 200  $\mu$ m underestimates the mesozooplankton abundance and community structure in this region (Feliú et al., 2020) and therefore we used the 50  $\mu$ m mesh size. Filtered volume was measured using a mechanical flow meter (Hydro-Bios, Germany). The raw oceanographic data are publicly available at the ISRAMAR oceanographic database website (<http://isramar.ocean.org.il>, last access: May 2022).

### 2.2 SeaExplorer glider mission to characterize the physical characteristics of the water column (upper 700 m) within and outside the core area

An autonomous underwater vehicle (SeaExplorer glider, ALSEAMAR) equipped with a Seabird CTD was deployed at the southernmost sampling station (at the core of the anticyclone). The glider collected the temperature and salinity characteristics across the upper 700 m in a very high spatiotemporal coverage during  $\sim$  18 d. The glider performed a total of 146 dives on its route northwards, yielding 292 quasi vertical profiles (see the glider track in Fig. 1a).

### 2.3 Inorganic nutrients

Nutrient concentrations were determined using a three-channel segmented flow auto-analyzer system (AA-3 Seal

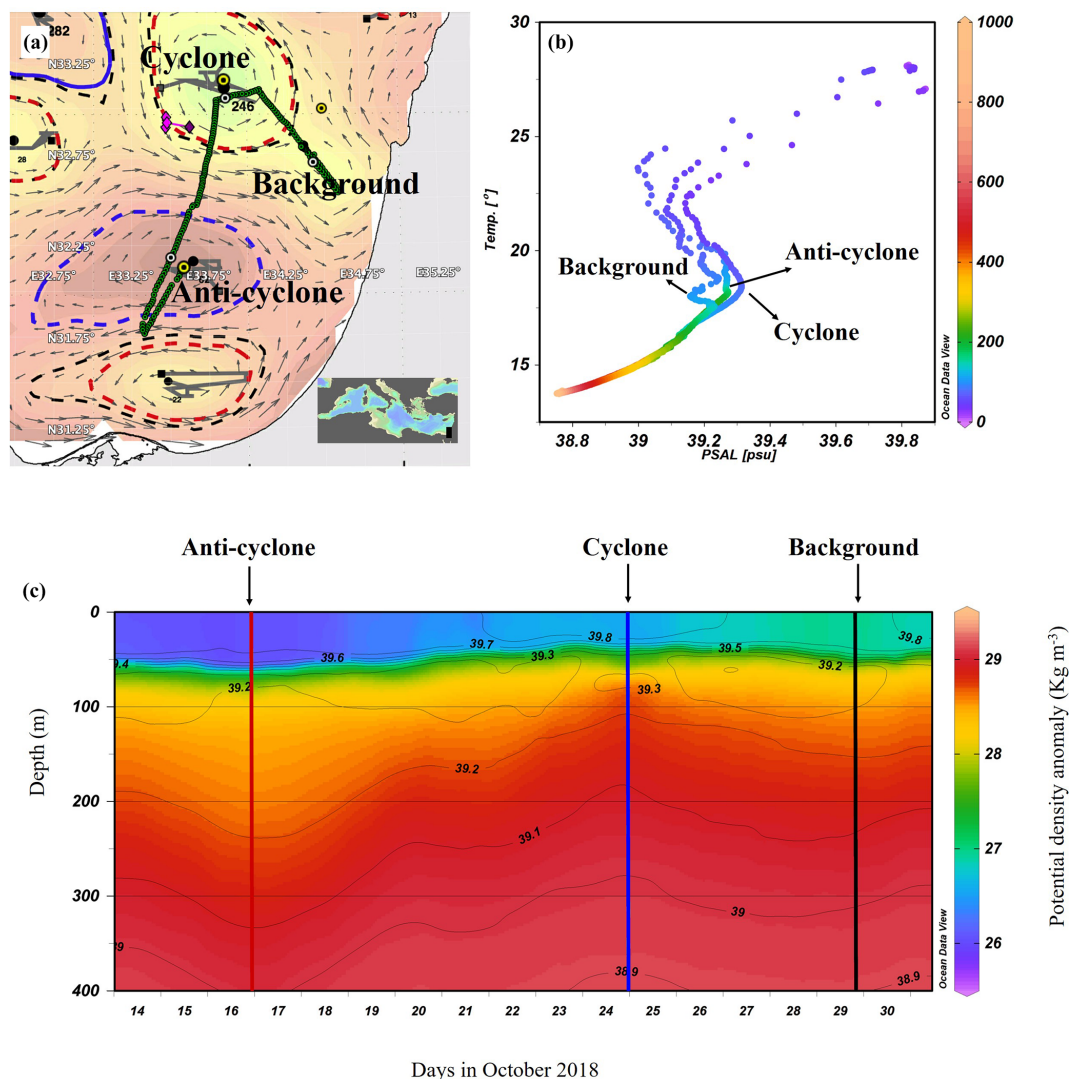


**Figure 1.** Altimetry map with eddies detected by the AMEDA algorithm created on the morning of the cruise (9 October 2018): sampling stations (yellow marks) and a glider cruise track (green dots) (a), temperature–salinity ( $T-S$ ) diagram of the stations sampled (b), and the potential density anomaly derived from a glider mission (292 quasi-vertical profiles) held a few days after the cruise (13–31 October 2018) (c). Contours on the density map show the corresponding isohalines.

Analytical) as described in Sisma-Ventura and Rahav (2019). The detection limit (3 times the standard deviation of 10 measurements of low-nutrient seawater), was  $0.08 \mu\text{mol L}^{-1}$  for  $\text{NO}_2 + \text{NO}_3$  ( $\text{NO}_x$ ),  $0.008 \mu\text{mol L}^{-1}$  for  $\text{PO}_4^{3+}$  and  $0.05 \mu\text{mol L}^{-1}$  for  $\text{Si}(\text{OH})_4$ . Analysis reproducibility was determined using MOOS 3 ( $\text{PO}_4^{3+}$ ,  $\text{NO}_x$  and  $\text{Si}(\text{OH})_4$ ), VKI 4.1 ( $\text{NO}_x$ ) and VKI 4.2 ( $\text{PO}_4^{3+}$  and  $\text{Si}(\text{OH})_4$ ) certified references materials (CRMs). Results were accepted when measured CRMs were within  $\pm 5\%$  from the certified values.

## 2.4 Chlorophyll $a$ and algal photosynthetic pigments markers

Seawater samples (500 mL) were concentrated on deck using a Whatman GF/F ( $\sim 0.7 \mu\text{m}$  pore size) at low pressure ( $< 150 \text{ mbar}$ ) for chlorophyll  $a$  (chl  $a$ ) analysis. The filters were placed in glass vials and frozen in the dark at  $-20^\circ\text{C}$  until analysis. Chl  $a$  pigment was extracted overnight in cold acetone (90 %) in the dark and determined by the non-acidification method (Welschmeyer, 1994) using a Turner Designs (Trilogy) fluorometer. The chl  $a$  reads were then calibrated against the in situ fluorimeter mounted on the rosette, using a linear regression equation ( $n = 19$ ,  $r = 0.95$ ,  $p < 0.001$ ). For biomarker photosynthetic pigment analyses,

8 L of seawater was concentrated on GF/Fs and kept frozen at  $-20^{\circ}\text{C}$  in aluminum foil until analysis. High-performance liquid chromatography (HPLC) was used to identify and quantify the biomarker photosynthetic pigments concentrations using a 40 min ethyl-acetate methanol gradient method (Jeffrey et al., 1997). Pigments were extracted in 90 % acetone for 24 h in  $4^{\circ}\text{C}$ . The extracts were filtered through a  $0.45\ \mu\text{m}$  Teflon syringe filter and transferred into glass HPLC vials. The extracts ( $100\ \mu\text{L}$ ) were analyzed using an Agilent 1220 HPLC system equipped with a diode array and fluorescence detectors. Selected pigment standards (DHI Labs) were used for verification of the spectra and retention times.

## 2.5 Pico-/nano-phytoplankton and heterotrophic prokaryotic abundance

Samples ( $1.8\ \text{mL}$ ) were fixed with glutaraldehyde (final concentration  $0.02\ \% v : v$ , Sigma-Aldrich G7651), frozen in liquid nitrogen, and later stored at  $-80^{\circ}\text{C}$  until analysis within 1 week. The abundance of autotrophic pico- and nano-eukaryotes, *Synechococcus* and *Prochlorococcus*, and other heterotrophic prokaryotes (bacteria and archaea) was determined using an Attune<sup>®</sup> Acoustic Focusing Flow Cytometer (Applied Biosystems). Heterotrophic prokaryotes (hereafter refer to as heterotrophic bacteria, BA) were stained with SYBR Green (Applied Biosystems). Total phytoplankton and microbial biomass was calculated according to Houlbrèque et al. (2006). Phytoplankton and microbial doubling time estimates were calculated by dividing the integrated phytoplankton biomass by integrated primary and bacterial production, respectively (Kirchman, 2012).

## 2.6 Primary production (PP)

Triplicate water samples ( $50\ \text{mL}$ ) were spiked upon sampling with  $5\ \mu\text{Ci}$  of  $\text{NaH}^{14}\text{CO}_3$  (Perkin Elmer, specific activity  $56\ \text{mCi mmol}^{-1}$ ) (Steeemann-Nielsen, 1952). The samples were incubated for 24 h under in situ natural illumination and surface temperature in a flow-through tank on deck covered with a light screening mesh. The incubations were terminated by filtering the spiked seawater through GF/F filters (Whatman,  $0.7\ \mu\text{m}$  pore size) at low pressure ( $\sim 50\ \text{mmHg}$ ). Measurements for the added activity and dark controls were also performed. The filters were placed overnight in  $5\ \text{mL}$  scintillation vials containing  $50\ \mu\text{L}$  of 32 % hydrochloric acid to remove excess  $^{14}\text{C}$ , after which  $5\ \text{mL}$  of scintillation cocktail (Ultima-Gold) were added. Radioactivity was measured using a TRI-CARB 2100 TR (Packard) liquid scintillation counter.

Note that the rates considered here only account for the particulate PP and not the dissolved fraction, and therefore the total PP may be underestimated (by an average of  $\sim 20\ \%$  in oligotrophic seas, Marañón et al., 2005). Yet we surmise that if underestimation did occur, it was similar at all stations sampled. Moreover, it is to be noted that due to the relatively

low number of depths sampled at each station ( $n = 5\text{--}6$ ), it is possible that some peaks in PP (e.g., at the subsurface) may have been overlooked, resulting in an underestimation of the integrated values.

## 2.7 Bacterial production (BP)

Prokaryotic (bacteria and archaea) heterotrophic production (hereafter refer to as BP) was estimated using the  $^3\text{H}$ -leucine incorporation method (Perkin Elmer, specific activity  $100\ \text{Ci mmol}^{-1}$ ). Three replicates ( $1.7\ \text{mL}$  each) from each water depth were incubated in the dark (wrapped in aluminum foil) with  $\sim 10\ \text{nmol}$  hot leucine  $\text{L}^{-1}$  for 4 h (Rahav et al., 2019). Control treatments in which surface water was immediately added with  $100\ \mu\text{L}$  of 100 % trichloroacetic acid (TCA,  $4^{\circ}\text{C}$ ) along with  $^3\text{H}$ -leucine were also carried out in triplicates. The incubations were terminated with TCA and were later processed following the micro-centrifugation technique (Smith et al., 1992) and added with  $1\ \text{mL}$  of scintillation cocktail (Ultima-Gold). The samples were counted using a TRI-CARB 2100 TR (Packard) liquid scintillation counter. A conversion factor of  $1.5\ \text{kg C mol}^{-1}$  per every mole leucine incorporated was used (Simon et al., 1989).

## 2.8 Zooplankton biomass

Zooplankton samples were sieved through a  $100\ \mu\text{m}$  mesh and halved into two subsamples using a plankton sample splitting box (Motoda, 1959). One subsample was kept at  $-20^{\circ}\text{C}$  for biomass analysis and the second subsample was preserved in 99.8 % ethanol for molecular analysis (Harris et al., 2000). In the lab, the collected samples were thawed and filtered using pre-combusted GF/C filters and weighed after drying in  $60^{\circ}\text{C}$  for 24 h to obtain dry weight (DW) and after 4 h in  $500^{\circ}\text{C}$  to measure ash weight and obtain carbon content as ash-free dry weight (AFDW).

The grazing impact of zooplankton on phytoplankton was calculated as the relative portion of zooplankton carbon biomass from the total pico-/nano-phytoplankton biomass (Feliú et al., 2020).

## 2.9 Zooplankton carbon and nutrient demand estimates

Zooplankton carbon demand (ZCD in  $\text{mg C m}^{-3}\ \text{d}^{-1}$ ) was calculated based on measured biomass and growth rate estimates (following the cross-Mediterranean estimates in Feliú et al., 2020):

$$\text{ZCD} = C_{\text{zoo}} \times F_{\text{R}},$$

where  $C_{\text{zoo}}$  is the carbon concentration of zooplankton (in  $\text{mg C m}^{-3}$ ) and  $F_{\text{R}}$  is the food ratio, defined as the amount of food consumed per unit of biomass per day ( $\text{d}^{-1}$ ), calculated as

$$F_{\text{R}} = \frac{gz + r}{A},$$

where  $g_Z$  is the growth rate,  $r$  is the weight specific respiration and  $A$  is assimilation efficiency.  $r$  and  $A$  were set to  $0.16 \text{ d}^{-1}$  following Alcaraz et al. (2007) and 0.7 following Nival et al. (1975).  $g_Z$  was calculated following Zhou et al. (2010):

$$g_Z(C_{Z00}, T, \text{chl } a) = 0.033 \left( \frac{\text{chl } a}{\text{chl } a + 205e^{-0.125T}} \right) e^{0.09T} \times W_{Z00}^{-0.06},$$

where  $T$  is seawater temperature (average value for 0–300 m: background  $18.8^\circ\text{C}$ , cyclone  $17.8^\circ\text{C}$ , anticyclone  $20.0^\circ\text{C}$ ) and  $\text{chl } a$  is food availability ( $\text{mg C m}^{-3}$ ) estimated from the integrated  $\text{chl } a$  values.  $W_{Z00}$  is the average carbon concentration per zooplankton, set to  $0.01072 \text{ mg C per individual}$  based on data collected from the background station in 2019–2020 (Guy-Haim, unpublished data). Phytoplankton was regarded as food following Calbet et al. (1996). ZCD was compared to the phytoplankton stock and to primary production to estimate the potential clearance of phytoplankton by zooplankton.

N and P excretion and oxygen consumption rates for an average zooplankton with weight  $W_{Z00}$  were estimated using the multiple regression model by Ikeda (1985) based on carbon weight and temperature:

$$\ln Y = a_0 + a_1 \ln W_{Z00} + a_2 T,$$

where  $Y$  represents N or P excretion or oxygen uptake.  $a_0$ ,  $a_1$  and  $a_2$  are constants specific to each metabolic process (respiration, ammonia and phosphate excretion). Total N and P excretion were obtained by multiplying the obtained rate with the zooplankton biomass measured at each station. Zooplankton's contribution to nutrient regeneration (in %) was estimated by comparison to primary production converted to N and P requirements. To this end, we used C : N : P ratios different than the “typical” Redfield 106 : 16 : 1 stoichiometry as previously reported in the ultra-oligotrophic Levantine Basin water (Pujo-Pay et al., 2011), where the particulate organic carbon (POC) to particulate nitrogen (PN) ratio (POC : PN) is 5.4 : 1 (instead of  $\sim 6.6 : 1$ ) and POC : PP is 116 : 1 (instead of 106 : 1). Respiration was converted to respiratory carbon lost assuming a respiratory quotient of 0.97 following Ikeda et al. (2000) and used as a carbon requirement for zooplankton metabolism.

## 2.10 Molecular diversity of microbial and zooplankton communities

Seawater (8L) was filtered using a peristaltic pump onto Supor membrane filters ( $0.2 \mu\text{m}$ , 47 mm, PALL, USA) and placed immediately in PowerWater DNA bead tubes (Qiagen, USA), flash-frozen in liquid nitrogen and preserved at  $-20^\circ\text{C}$  ( $n = 1$  per depth except in selected samples where  $n = 2$ ). DNA was extracted with the DNeasy PowerWater

Kit (Qiagen, USA), following the standard protocol including an extra heating step at  $65^\circ\text{C}$  for 10 min as recommended by the manufacturer for samples containing algae. Ethanol-preserved zooplankton samples were sieved using a  $100 \mu\text{m}$  Nitex sieve, washed with distilled water to remove ethanol residuals, and homogenized by vigorous vortex and pipetting. Genomic DNA was extracted using DNeasy Blood and Tissue Kit (Qiagen, USA) following the manufacturer's instructions.

DNA was amplified with the following primer sets amended with CS1/CS2 tags: (i) the V4 region of the 16S rRNA gene (ca. 300 bp), 515Fc/806Rc (Apprill et al., 2015; Parada et al., 2016); (ii) the 18S rRNA gene (200–500 bp), 1391F, EukBr (Amaral-Zettler et al., 2009); and (iii) the mitochondrial cytochrome *c* oxidase I (COI) gene (ca. 300 bp), mICOIntF, jgHCO2198. Library preparation from the PCR products and sequencing of  $2 \times 250 \text{ bp}$  Illumina MiSeq reads were performed by HyLabs (Israel). The COI and 18S rRNA gene amplicon reads were submitted to NCBI Sequence Read Archive BioProject PRJNA667077.

## 2.11 Bioinformatic analyses of marker gene amplicons

Demultiplexed paired-end reads were processed in a QIIME2 V2020.6 environment (Bolyen et al., 2019). Reads were truncated based on quality plots, checked for chimeras, merged and grouped into amplicon sequence variants (ASVs) with DADA2 (Callahan et al., 2016), as implemented in QIIME2. The 16S and 18S rRNA amplicons were classified with a scikit-learn classifier that was trained on the Silva 138 database or BLAST against the Silva 138 database (0.9 minimum identity cutoff, performed best for the analyses of 18S gene amplicons of microbial zooplankton). COI amplicons were classified with BLAST (0.9 minimum identity cutoff) against the merged NCBI/BOLD database (Heller et al., 2018), which was transformed into QIIME2 format. Downstream statistical analyses, calculation of alpha diversity indices (the richness estimator ACE, Abundance-based Coverage Estimator, and the biodiversity estimators Shannon and Simpson), beta diversity (non-metric multidimensional scaling, NMDS, based on the Bray–Curtis dissimilarity) and plotting were performed in R (R Core Team, 2018) using packages phyloseq (McMurdie and Holmes, 2013), ampvis2 (Andersen et al., 2018) and ggplot2 (Wickham, 2011). Mitochondrial and chloroplast sequences were removed from the 16S rRNA amplicon dataset, and the relative abundance of microbial eukaryotes was estimated following the removal of metazoan 18S rRNA sequences.

## 2.12 Statistical analyses

Nutrients, pico-phytoplankton, heterotrophic bacteria, and primary and bacterial production were vertically integrated using the trapezoidal rule and compared between sampling locations (“background”, “anticyclonic eddy” and “cyclonic

eddy”) using a one-way analysis of variance (ANOVA) and a Fisher’s least significant difference (LSD) means comparison test ( $\alpha = 0.05$ ). Statistically significant differences ( $p < 0.05$ ) were labeled with different letters. DESeq2 (Love et al., 2014) was used to evaluate the differential abundance of bacterioplankton ASVs at the deep chlorophyll maximum (DCM). Note that the limited number of samples collected in each hydrologic discontinuity per depth ( $n = 1\text{--}2$ ), contrary to integrated calculations which pool four to six measurements from the upper 180 m, restricted our ability to run additional statistical comparisons between locations. We discuss these caveats below and also compare our findings to other relevant studies from the Mediterranean Sea (i.e., the BOUM and ISRALEV campaigns) and elsewhere (e.g., the eastern Indian Ocean, Waite et al., 2007) and compare our nutrients and chl *a* profiles to a parallel cruise held at the same time as our study nearby (Fig. S1).

### 3 Results

The AMEDA algorithm shows a chain of cyclonic and anticyclonic eddies at the SEMS (Fig. 1a). The stations were selected to sample the cores of the southern cyclonic and anticyclonic eddies offshore the Israeli coast as well as background stations. The anticyclone, later identified in the DYNED atlas as anticyclone no. 12683, was created from a meander of the along-shore current in the southeastern corner of the basin in early August 2018, just 62 d prior to the cruise. It mixed warm water from the eastern sea margin (Fig. S2A in the Supplement). The cyclonic eddy was created in early February 2018, 246 d before the cruise. Later, when the DYNED atlas was extended to include 2018, it was identified as cyclonic eddy no. 11988, which was created more than a year earlier in mid-September 2017 (Fig. S2 in the Supplement). It was split from cyclone no. 11310 located south of Cyprus and migrated to the easternmost SEMS. Profiles of Argo floats (no. 6903221 and no. 6903222) localized within cyclone no. 11310 showed that it brought denser, colder and saltier water upwelled on the southern Cyprus coast (Fig. S2A). At the time it was sampled it is characterized as a cold-core cyclone, colder than its surrounding waters (Fig. S2B in the Supplement).

The sea surface temperature (SST) at the anticyclonic eddy and background stations was the warmest ( $\sim 28^\circ\text{C}$ ), while a lower temperature was recorded in the cyclonic eddy ( $\sim 27^\circ\text{C}$ ) (Figs. 1b and S3 in the Supplement). Further, down to 550 m the highest water temperatures were recorded in the anticyclonic eddy (a positive anomaly compared to the background), and the coldest temperatures were recorded in the cyclonic eddy (a negative anomaly). From  $\sim 550$  to 1000 m depth the water temperature at all sampling stations was the same and constant ( $\sim 14^\circ\text{C}$ ) (Fig. S3). Surface salinity ranged from 39.7 to 39.8 psu and decreased to 38.8 psu at 550 m in all sampling sites (Figs. 1b and S3). The concurrent

potential density anomaly derived from a detailed glider mission that occurred in the week following our cruise and shows that the sampling stations were within the cores of the two distinct hydrologic discontinuities (Fig. 1c). The Levantine Intermediate Water (LIW), characterized by high salinity and relatively warm temperatures, was evident at  $\sim 70$  m in the upwelling cyclonic eddy,  $\sim 130$  m at the background station and  $\sim 170$  m at the downwelling anticyclonic site (Fig. 1b). This means that at the core of the cyclone, the LIW mass was uplifted to a relatively narrow layer (50–80 m; core at 75 m), while in the core of anticyclone the LIW was much wider and deeper (80–240 m; core 175 m) due to the convergence of currents (Fig. S3).

$\text{NO}_2^- + \text{NO}_3^-$  ( $\text{NO}_x$ ) and orthophosphate ( $\text{PO}_4^{3+}$ ) concentrations were close to, or below, the detection limit of conventional analytical methods at all stations in the upper 100 m, while  $\text{Si}(\text{OH})_4$  levels were always above the detection limit (Fig. 2a–c, Table S1 in the Supplement). Nevertheless, marked differences were observed in the integrated nutrient values between sites in the photic layer (0–180 m), with 13-fold higher  $\text{NO}_x$ , 2.5-fold higher  $\text{PO}_4^{3+}$  and 1.5-fold higher  $\text{Si}(\text{OH})_4$  in the cyclonic eddy compared with the anticyclone (Table 1). Integrated N : P ratios at the background and anticyclone stations were lower than the Redfield ratio (15 : 1 and 9 : 1, respectively), whereas in the cyclone the N : P ratio was higher ( $\sim 48$  : 1) (Table 1). From 180 m and down to the nutricline shoulder ( $\sim 400$  m), all nutrient levels gradually increased.  $\text{NO}_x$ ,  $\text{PO}_4^{3+}$  and  $\text{Si}(\text{OH})_4$  were higher by 45 %, 90 % and 100 % in the cyclonic eddy than the anticyclonic eddy, respectively (Fig. 2a–c, Table S1).

Following the elevated nutrient levels, integrated chl *a* was highest in the cyclonic eddy and at background stations ( $20.0\text{--}21.3 \text{ mg m}^{-2}$ ) and lowest at the center of the ultra-oligotrophic anticyclonic eddy ( $17.9 \text{ mg m}^{-2}$ ) (Tables 1 and S1). The deep chlorophyll maximum (DCM) spread from 90–120 m in the cyclonic eddy, while a smaller DCM shoulder was observed in the anticyclonic eddy ( $\sim 90\text{--}120$  m) and at the background ( $\sim 120\text{--}130$  m) stations (Fig. 3a). Nonetheless, the cyclone had the highest chl *a* concentration among all stations ( $0.31 \mu\text{g L}^{-1}$ ), while the DCM in the anticyclonic eddy had a weaker chl *a* signal ( $0.18 \mu\text{g L}^{-1}$ ) (Fig. 3a, Table S1). *Synechococcus* was mostly found in the surface water of all stations, whereas *Prochlorococcus* occupied the DCM depths (Fig. 3b and c). The highest cell abundance of these cyanobacteria was found at the background station ( $69 \times 10^{10}$  *Synechococcus* cells  $\text{m}^{-2}$ ) and in the anticyclone ( $270 \times 10^{10}$  *Prochlorococcus* cells  $\text{m}^{-2}$ ), while the lowest abundances were found in the cyclone ( $\sim 27 \times 10^{10}$  *Synechococcus* cells  $\text{m}^{-2}$  and  $\sim 160 \times 10^{10}$  *Prochlorococcus* cells  $\text{m}^{-2}$ ) (Tables 1 and S1). Cyanobacterial read abundance based on amplicon sequencing supported these findings (Fig. 4). The dominant bacterioplankton lineages in the photic zone included SAR86, Flavobacteriales, Punicespirillales, Rhodospirillales and SAR11 (clade Ia) (Figs. 4 and S4). The abundance

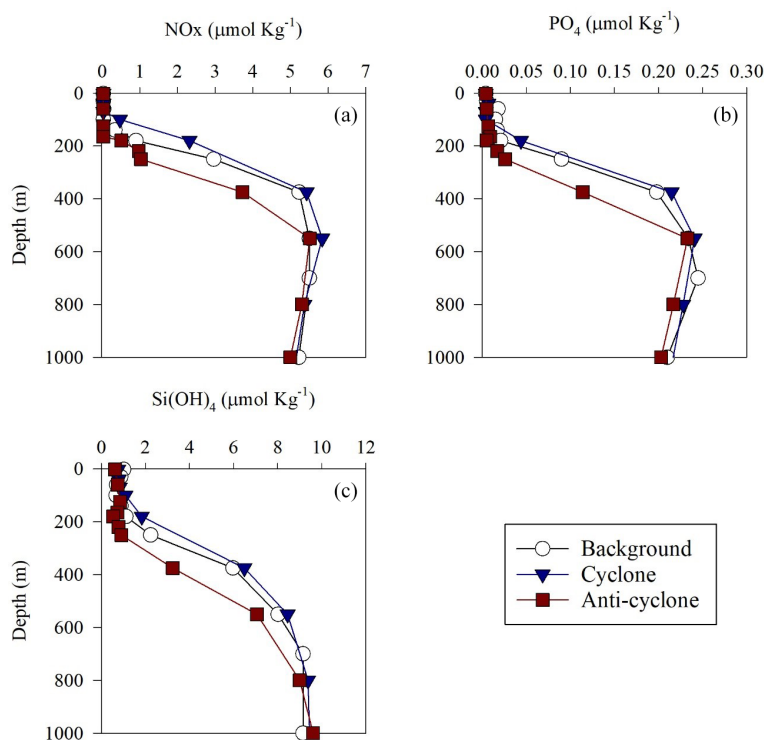


**Figure 2.** Vertical profile of  $\text{NO}_x$  (a),  $\text{PO}_4^{3+}$  (b) and  $\text{Si(OH)}_4$  (c) in cyclonic (blue triangle) and anticyclonic (red square) eddies and an uninfluenced background station (white circle) in the southeastern Mediterranean Sea during October 2018.

of pico- and nano-eukaryotic phytoplankton was higher at the cyclonic station ( $13.5 \times 10^{10}$  cells  $\text{m}^{-2}$ ) than the other stations sampled ( $\sim 5.5 \times 10^{10}$  cells  $\text{m}^{-2}$ ) (Tables 1 and S1). Pico-eukaryotes were mostly found in the surface water (top 50 m) and nano-eukaryotes were mostly found at the DCM depth (Fig. 3d and e). Correspondingly, total pico-phytoplankton biomass was highest in the cyclonic eddy ( $597 \text{ mg C m}^{-2}$ ), which is 1.6–1.7-fold higher than at the background or anticyclonic stations (Tables 1 and S1). The 18S rRNA amplicon analyses indicated that at the photic depths mainly non-diatom microbial eukaryotes were dominant, such as dinoflagellates, Prymnesiophyceae and Ochrophyta (Figs. 5 and S5). Overall, the pico- and nano-eukaryotic populations were more diverse in the photic zone than in the deep waters, yet no major differences in alpha diversity parameters were observed between the stations (Fig. S6).

Algal pigment analysis in the cyclone showed that the photosynthetic auxiliary pigments were mostly comprised of fucoxanthin ( $109 \text{ ng L}^{-1}$ ) – a pigment marker of diatoms, chrysophytes and some prymnesiophytes – and zeaxanthin ( $74 \text{ ng L}^{-1}$ ) – a pigment marker for green algae and cyanobacteria (Fig. S7). At the anticyclonic eddy, fucoxanthin was also detected at the DCM; however, its concentration was lower by  $\sim 40\%$  ( $\sim 65 \text{ ng L}^{-1}$ ), while the zeaxanthin concentration was slightly lower ( $\sim 64 \text{ ng L}^{-1}$ ) (Fig. S7). As very few diatoms were detected by the 18S

rRNA amplicon analysis, we surmise that the presence of fucoxanthin was most likely attributed to prymnesiophytes. Although the most considered diagnostic marker for prymnesiophytes is 19-hexanoyloxyfucoxanthin, previous studies showed that fucoxanthin can also be used as their marker in the absence of 19-hexanoyloxyfucoxanthin signals (Ansoategui et al., 2003).

Following the higher nutrients levels and pico-phytoplankton biomass, PP was highest in the cyclone ( $191 \text{ mg C m}^{-2} \text{ d}^{-1}$ ) and significantly decreased by 50%–80% at the background ( $81 \text{ mg C m}^{-2} \text{ d}^{-1}$ ) and anticyclone ( $36 \text{ mg C m}^{-2} \text{ d}^{-1}$ ) stations (Tables 1 and S1). The highest PP rates were found in the surface water of all stations ( $\sim 0.8$ – $2.0 \mu\text{g CL}^{-1} \text{ d}^{-1}$ ) and decreased with depth throughout the photic layer (Fig. 3f). The differences in the vertical distribution of chl *a* and PP were also evident in the assimilation number of phytoplankton, which signifies autotrophically specific activity (PP per chl-*a*). The assimilation number was highest in the cyclone ( $10 \text{ g C g chl } a^{-1} \text{ d}^{-1}$ ) and lower by 60%–80% at the anticyclone and background stations ( $2$ – $4 \text{ g C g chl } a^{-1} \text{ d}^{-1}$ ) (Tables 1 and S1). Integrated doubling times of pico-/nano-phytoplankton were highest at the anticyclone (9.7 d) and lowest in the cyclone (3.1 d) (Table 1).

Total BA was higher by 1–2 orders of magnitude than the pico-phytoplankton abundance (Fig. 6a, Table S1). The highest BA was measured at the anti-

**Table 1.** Chemical and biological integrated values at the upper 180 m (except zooplankton where 0–300 m is presented) measured at the different sampling sites. The maximal values for each variable are highlighted in bold.

Variable	Background	Cyclone	Anticyclone
NO <sub>x</sub> (mmol m <sup>-2</sup> )	35.5	<b>121.2</b>	9
PO <sub>4</sub> <sup>3+</sup> (mmol m <sup>-2</sup> )	2.4	<b>2.5</b>	1
N : P	15	<b>48</b>	9
Si(OH) <sub>4</sub> (mmol m <sup>-2</sup> )	150.2	<b>200.7</b>	133.3
Chl <i>a</i> (mg m <sup>-2</sup> )	<b>21.3</b>	20	17.9
<i>Synechococcus</i> (× 10 <sup>10</sup> cells m <sup>-2</sup> )	<b>69</b>	27	54
<i>Prochlorococcus</i> (× 10 <sup>10</sup> cells m <sup>-2</sup> )	231	163	<b>273</b>
Pico-eukaryotes (× 10 <sup>10</sup> cells m <sup>-2</sup> )	1.7	<b>7.2</b>	2.3
Nano-eukaryotes (× 10 <sup>10</sup> cells m <sup>-2</sup> )	3.3	<b>6.3</b>	3
Total pico-/nano-phytoplankton biomass (mg C m <sup>-2</sup> )	369	<b>597</b>	348
Heterotrophic bacteria (× 10 <sup>10</sup> cells m <sup>-2</sup> )	1459	2072	<b>2125</b>
Heterotrophic bacteria biomass (mg C m <sup>-2</sup> )	204	290	<b>298</b>
Zooplankton biomass (mg DW m <sup>-2</sup> )	360	<b>3045</b>	303
Zooplankton biomass (mg C m <sup>-2</sup> )	112	<b>1337</b>	133
Grazing impact on phytoplankton stock (%)	30	<b>224</b>	38
PP (mg C m <sup>-2</sup> d <sup>-1</sup> )	81	<b>191</b>	36
Assimilation number (g C g chl <i>a</i> <sup>-1</sup> d <sup>-1</sup> )	4	<b>10</b>	2
Phytoplankton doubling time (d)	4.6	3.1	<b>9.7</b>
BP (mg C m <sup>-2</sup> d <sup>-1</sup> )	82	<b>214</b>	85
Heterotrophic bacteria doubling time (d)	2.5	1.4	<b>3.5</b>
BP/BA (fg C cell <sup>-1</sup> d <sup>-1</sup> )	5.7	<b>10.3</b>	4.0
BP/PP	1.0	1.1	<b>2.4</b>
Zooplankton carbon demand (mg C m <sup>-2</sup> d <sup>-1</sup> )	34.3	<b>387.9</b>	41.8
Grazing impact on PP (%)	42	<b>203</b>	116
Zooplankton respiration (mg C m <sup>-2</sup> d <sup>-1</sup> )	14.8	<b>166.2</b>	18.9
% of PP respired by zooplankton	18	<b>87</b>	53
Zooplankton excretion (mg N-NH <sub>4</sub> m <sup>-2</sup> d <sup>-1</sup> )	2.2	<b>25</b>	2.9
Phytoplankton N demand (mg N m <sup>-2</sup> d <sup>-1</sup> )	17	<b>41</b>	8
% contribution of zooplankton N to PP	13	<b>61</b>	37
Zooplankton excretion (mg P-PO <sub>4</sub> m <sup>-2</sup> d <sup>-1</sup> )	0.3	<b>3.6</b>	0.4
Phytoplankton P demand (mg P m <sup>-2</sup> d <sup>-1</sup> )	1.8	<b>4.2</b>	0.8
% contribution of zooplankton P to PP	17	<b>85</b>	50

cyclone ( $2125 \times 10^{10}$  cells m<sup>-2</sup>) followed by the cyclonic eddy ( $2072 \times 10^{10}$  cells m<sup>-2</sup>) and background ( $1459 \times 10^{10}$  cells m<sup>-2</sup>) stations (Table 1). Contrary to the BA or biomass, BP was significantly higher at the cyclone ( $214 \text{ mg C m}^{-2} \text{ d}^{-1}$ ) compared to the anticyclone and background stations ( $82\text{--}85 \text{ mg C m}^{-2} \text{ d}^{-1}$ ) (Table 1). A similar trend was measured in heterotrophic bacteria cell-specific activity (BP/BA), where the most productive cells were found in the cyclone ( $10 \text{ fg C cell}^{-1} \text{ d}^{-1}$ ), while the least productive cells were found in the anticyclone ( $4 \text{ fg C cell}^{-1} \text{ d}^{-1}$ ) (Tables 1 and S1). Overall, BP was homogeneously distributed throughout the photic layer at all stations ( $\sim 0.2\text{--}0.9 \mu\text{g CL}^{-1} \text{ d}^{-1}$ ), except the cyclonic eddy where the rates were relatively high in the upper 100 m ( $\sim 0.8\text{--}2.4 \mu\text{g CL}^{-1} \text{ d}^{-1}$ ) (Fig. 6b). At 180 m, BP rates were similar at all stations ( $\sim 0.1 \mu\text{g CL}^{-1} \text{ d}^{-1}$ ) (Fig. 6b). The resulting BP/PP ratio was overall similar outside the

cyclone ( $\sim 1$ ) and was 2-fold higher inside it (Table 1). In accordance with the high BP, the integrated doubling time of heterotrophic bacteria was highest in the anticyclone (3.5 d) and lowest in the cyclone (1.4 d) (Table 1).

The slope of the log–log linear regressions for BA and BP obtained in the cyclonic eddy was 0.24 ( $R^2 = 0.60$ ), while in the anticyclonic eddy the slope was more than twice as high: 0.52 ( $R^2 = 0.79$ ) ( $P = 0.03$ , analysis of covariance, ANCOVA; Andrade and Estévez-Pérez, 2014).

In accordance with the high PP and BP, total zooplankton biomass in the upper 300 m was an order of magnitude higher in the cyclonic eddy ( $3045 \text{ mg DW m}^{-2}$ ,  $1337 \text{ mg C m}^{-2}$ ) compared with the anticyclonic ( $303 \text{ mg DW m}^{-2}$ ,  $133 \text{ mg C m}^{-2}$ ) or background ( $360 \text{ mg DW m}^{-2}$ ,  $112 \text{ mg C m}^{-2}$ ) stations (Tables 1 and S1). Zooplankton grazing impact on phytoplankton stock estimates shows that mesozooplankton consumed 30%–38% of the daily



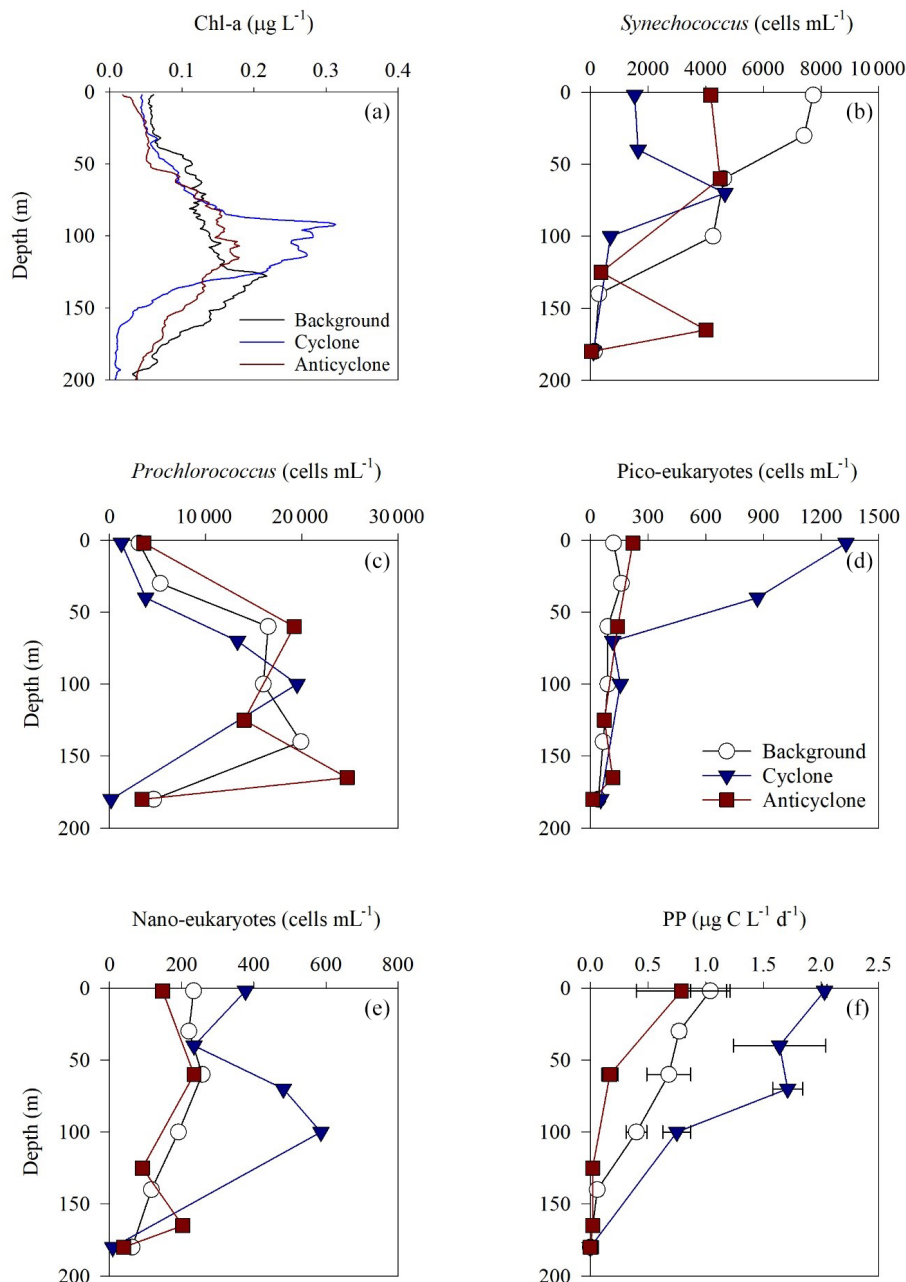


**Figure 3.** Vertical profile of chlorophyll *a* (a), *Synechococcus* (b), *Prochlorococcus* (c), pico-eukaryotes (d), nano-eukaryotes (e) and primary production rate (f) in the photic layer of cyclonic (blue triangle) and anticyclonic (red square) eddies and an uninfluenced background station (white circle) at the southeastern Mediterranean Sea during October 2018.

phytoplankton stock at the anticyclone and background stations and 224 % in the cyclone (Table 1). Similarly to zooplankton biomass, the estimated zooplankton carbon demand (ZCD) was highest in the cyclonic eddy ( $\sim 388 \text{ mg C m}^{-2} \text{ d}^{-1}$ ) and decreased by an order of magnitude at the anticyclonic eddy ( $\sim 42 \text{ mg C m}^{-2} \text{ d}^{-1}$ ) and the background ( $\sim 34 \text{ mg C m}^{-2} \text{ d}^{-1}$ ) stations (Tables 1 and S1). Considering phytoplankton as the major food source, zooplankton potentially consumed 203 % of PP in

the cyclonic eddy, 116 % in the anticyclonic eddy and only 42 % at the background station (Tables 1 and S1). Zooplankton respiration rates were 9–11-fold larger in the cyclone ( $\sim 166 \text{ mg C m}^{-2} \text{ d}^{-1}$ ) than at the anticyclone and background stations ( $\sim 15\text{--}19 \text{ mg C m}^{-2} \text{ d}^{-1}$ ), corresponding to 87 % vs. 18 %–53 % of the integrated PP (Tables 1 and S1). The estimated contribution of zooplankton to nitrogen regeneration by excretion of ammonium was 9–11-fold greater in the cyclone ( $25 \text{ mg N-NH}_4 \text{ m}^{-2} \text{ d}^{-1}$ ) than in the anticyclone

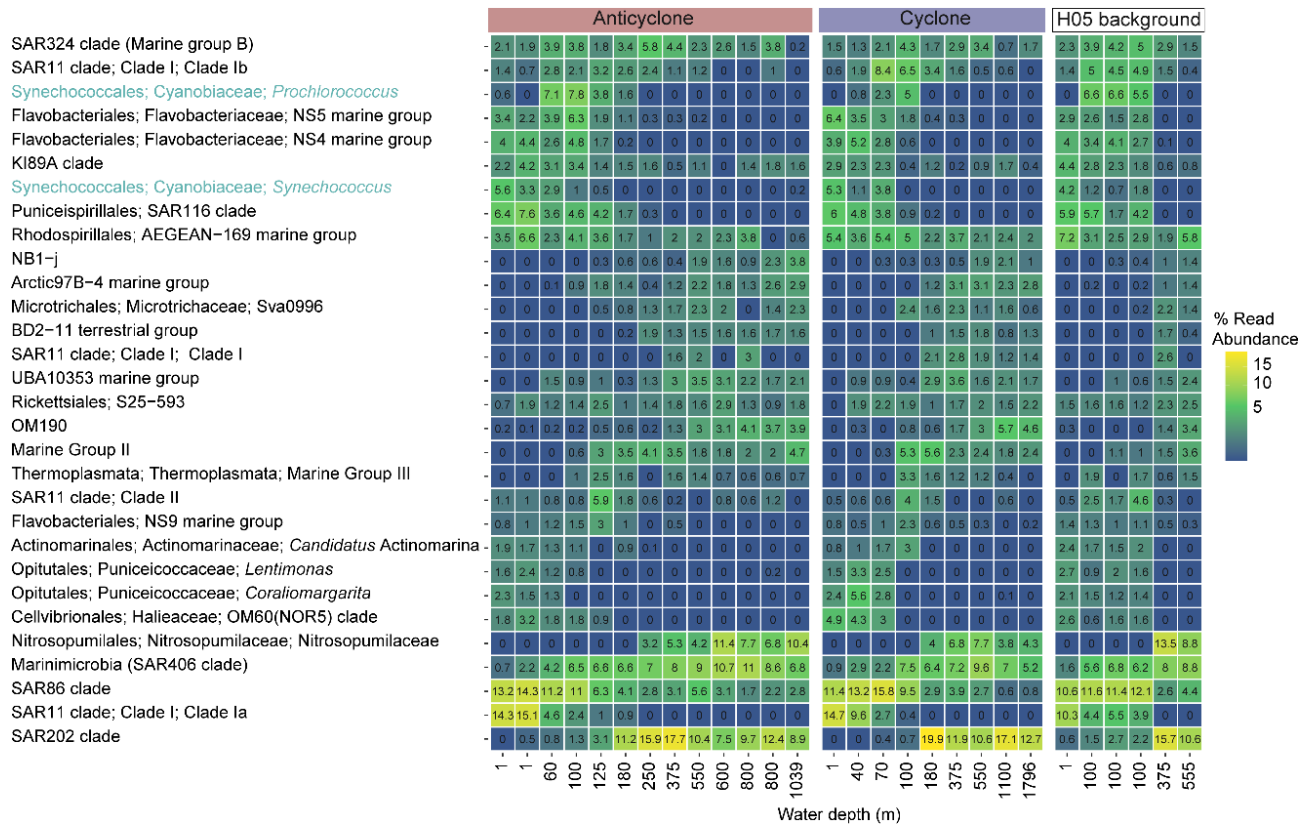


**Figure 4.** The relative abundance of the 30 most abundant bacterial and archaeal genera collected in cyclonic and anticyclonic eddies and an uninfluenced background station in the southeastern Mediterranean Sea during October 2018, as estimated by read abundance. Results of replicate casts at anticyclone and uninfluenced background (H05) stations are shown in columns with identical depths.

or the background stations ( $\sim 2\text{--}3 \text{ mg N-NH}_4 \text{ m}^{-2} \text{ d}^{-1}$ ), corresponding to 61 % vs. 13 %–37 % of the integrated PP (based on a C : N 5.4 : 1 ratio, Pujó-Pay et al., 2011) for the Levantine Basin water (Tables 1 and S1). The estimated contribution of zooplankton to phosphorus (as orthophosphate) by excretion was an order of magnitude greater in the cyclone ( $3.6 \text{ mg P-PO}_4 \text{ m}^{-2} \text{ d}^{-1}$ ) than at the anticyclone and background stations ( $0.3\text{--}0.4 \text{ mg P-PO}_4 \text{ m}^{-2} \text{ d}^{-1}$ ), corresponding to 85 % vs. 17 %–50 % of the integrated PP (based on a C : P 116 : 1 ratio, Pujó-Pay et al., 2011) (Tables 1 and S1).

Zooplankton alpha diversity estimated based on the COI and 18S rDNA genes read abundance as well as on cell abundance (i.e., microscopic identification) was highest at the cyclone and background stations and lowest in the anticyclone (Fig. 7). COI and 18S ASV richness (ACE index) were lowest in the anticyclone (29 and 81, respectively) and 60 % (18S) to 250 % (COI) larger at the cyclone and background stations (Fig. 7). The lowest zooplankton biodiversity (Shannon and Simpson indices) was found in the anticyclone, using both genes (Fig. 7). These findings were confirmed with rarefaction curves (Figs. S8 and S9 in the Supplement).

Classification to species level was successful in 211 out of 221 COI ASVs and in only 55 out of 830 18S ASVs, 200 of which were classified to an order level. The three stations differed in the zooplankton relative richness (i.e., the number of ASVs per taxonomical functional group) (Fig. 8). Overall, at all stations, copepods (Hexanauplia) were the most diverse group; nevertheless, copepod richness was 7-fold larger in the cyclone vs. the anticyclone. Ostracods and hydrozoans (mainly siphonophores) had a higher diversity at the background station than at the other stations. Chaetognaths, branchiopods (cladocerans), planktonic decapods and amphipods had similar richness levels at the cyclonic eddy and background stations; however, they were completely absent in the anticyclone. In contrast, a higher richness of gastropods (mainly pteropods) was found in the anticyclone compared to the cyclone and background stations. Although the majority of the taxonomic groups was better represented by COI classification, one group – Polychaeta – was better represented in the 18S rRNA (2 versus 12 ASVs), as 18S is more often used to obtain resolved phylogenies in polychaetes (Colgan et al., 2006). Based on the 18S rRNA gene ASVs, the highest richness of polychaetes was found at the cyclone (6 ASVs) and

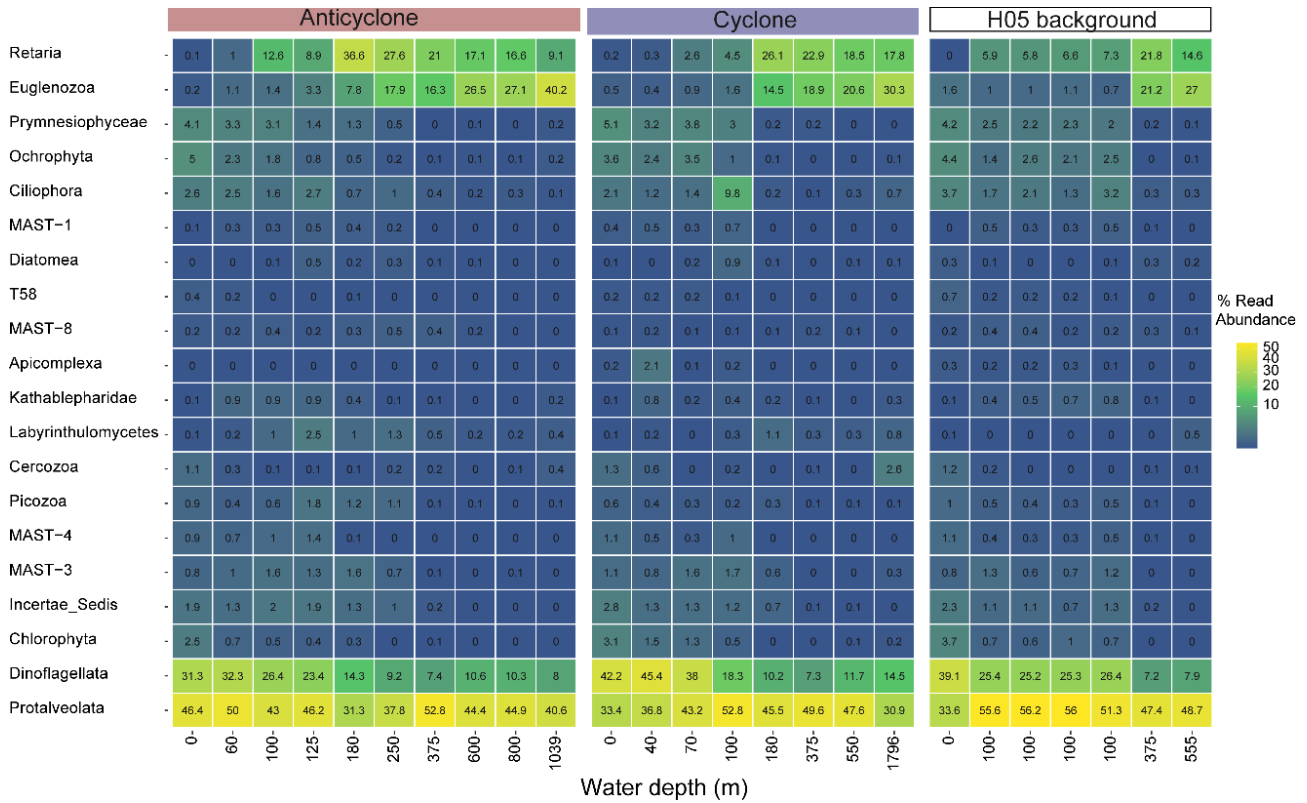


**Figure 5.** The relative abundance of the 20 most abundant unicellular eukaryotic lineages (phylum level), collected in cyclonic and anticyclonic eddies and at an uninfluenced background station (H05) in the southeastern Mediterranean Sea during October 2018, as estimated by read abundance. Results of replicate casts at anticyclone and control H05 stations are shown.

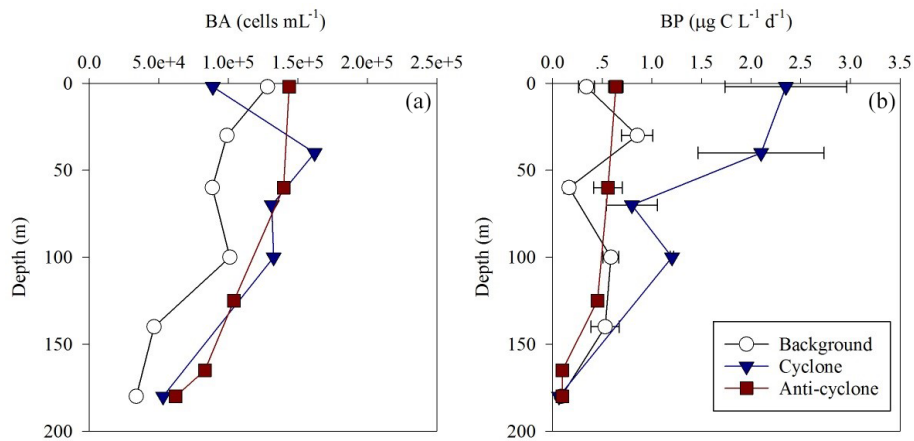


**Figure 6.** Vertical profile of heterotrophic bacterial abundance (a) and bacterial production rates (b) in the photic layer of cyclonic (blue triangle) and anticyclonic (red square) eddies and an uninfluenced background station (white circle) in the southeastern Mediterranean Sea during October 2018.

background (5 ASVs) stations, whereas only 2 ASVs were found in the anticyclone.

#### 4 Discussion

Seasonality is the primary driver affecting water column characteristics in the SEMS, where external inputs of nutrients such as from the atmosphere (Herut et al., 2002, 2005; Ridame et al., 2011) or large rivers (Ludwig et al., 2009)

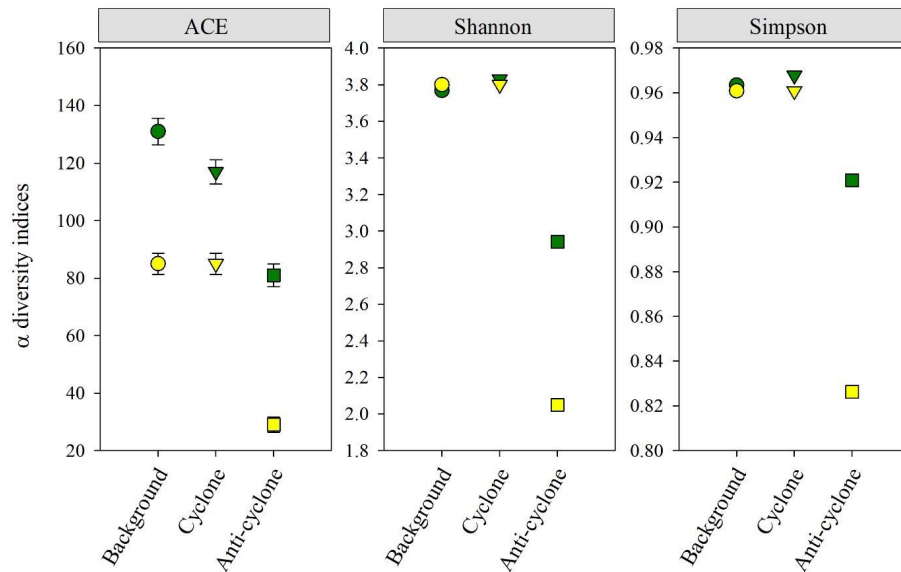


**Figure 7.** Zooplankton alpha diversity indices (ACE  $\pm$  SE, Shannon, Simpson) based on 18S (green) and COI (yellow) amplicon sequencing in  $> 100 \mu\text{m}$  samples collected from the upper 300 m of cyclonic and anticyclonic eddies and at an uninfluenced background station in the southeastern Mediterranean Sea during October 2018.

are limited in space and time. Thus, the one-dimensional processes of summer stratification and winter mixing determine, to a large extent, the nutrient availability in the photic layer ( $< 180 \text{ m}$ ), subsequently affecting phytoplankton population dynamics and activity (Van-Ruth et al., 2020). However, horizontal variability plays an important role. Turbulent mesoscale eddies are a prominent part of the circulation in the SEMS (Mkhinini et al., 2014). Such features have lifetimes of a few months to a year (Mkhinini et al., 2014), affecting the availability of the nutrients to phytoplankton and bacteria in the photic layer (Rahav et al., 2013; Vaillancourt et al., 2003) and thus to higher trophic levels (Dolan et al., 2002; Siokou-Frangou, 2004). The degree to which an eddy affects the community depends on the eddy's size, age, the source of the water “trapped” within it, and the interaction with wind and land (Gaube et al., 2014; Huggett, 2014; Landry et al., 2008a; Strzelecki et al., 2007). Our results demonstrate that upwelling within the cyclone injected deeper-water nutrients into the quasi-permanent eddy, thus fertilizing the planktonic population.

The effect of hydrodynamic structures on planktonic microbial distribution has been studied previously in the SEMS. However, these studies focused on long-lived anticyclonic eddies such as the Cyprus/Shikmona Eddy ( $> 6$  months, Christaki et al., 2011; Rahav et al., 2013; Thingstad et al., 2005). There is a strong asymmetry in an eddy's lifetime, which on average is far shorter for cyclones than anticyclones. This asymmetry is enhanced in the SEMS where the cyclone lifetime distribution is very similar to the rest of the Mediterranean Sea, yet the anticyclones live longer (Mkhinini et al., 2014). It makes the comparison of cyclones

and anticyclones more challenging in the SEMS as they are not circulating (and thus isolated) for the same time. We sampled a recent anticyclone (no. 12683, 2 months old) and a more “mature” cyclone (no. 11988, over 1 year old), which is not the usual scenario in the SEMS. The short-lived anticyclone and the background station do indeed have similar characteristics. We expect long-lived anticyclones to be even more oligotrophic, making their influence more prominent, as discussed below.

#### 4.1 Pico-phytoplankton dynamics and primary production in anticyclonic and cyclonic waters

Our results show that nutrient availability affected the pico-phytoplankton dynamics in the SEMS. The low pico-eukaryote biomass and the low N : P in the anticyclonic eddy ( $\sim 9 : 1$ ) suggest N limitation for these autotrophs under extreme oligotrophic conditions (Table 1). By contrast, the high N : P ratio ( $\sim 48 : 1$ ) and the relatively low cyanobacterial biomass in the cyclonic eddy suggest that *Synechococcus* and *Prochlorococcus* are P-limited. These results are similar to a previous study from the SEMS showing that  $\text{NO}_x$  concentrations at the Rhodes Gyre (upwelling) were 5-fold higher than in the Cyprus Eddy (downwelling), while  $\text{PO}_4^{3+}$  remained similarly low for the two locations (Rahav et al., 2013). These variations result in significant differences in the  $\text{NO}_x : \text{PO}_4^{3+}$  ratio of the two systems, the Rhodes Gyre ( $\sim 50 : 1$ ) and the Cyprus Eddy ( $\sim 10 : 1$ ), implying similar nutrient limitations as discussed above. The stoichiometric N : P Redfield ratio alone, however, cannot fully explain which nutrients limit the microbial plankton diversity. Some

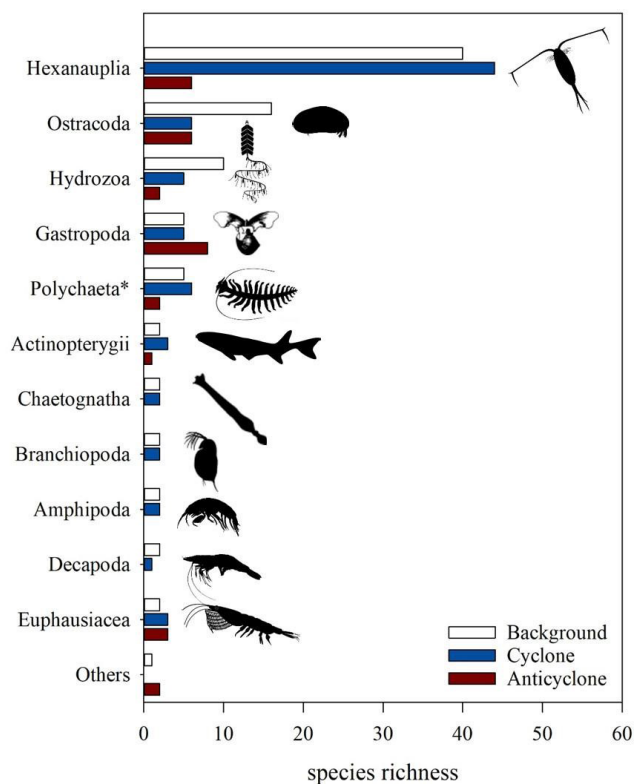


**Figure 8.** Zooplankton species richness based on COI amplicon sequences (classified using a BOLD/NCBI-based database) in  $> 100 \mu\text{m}$  samples collected from the upper 300 m of cyclonic and anticyclonic eddies and at an uninfluenced background station in the southeastern Mediterranean Sea during October 2018. Polychaeta richness was obtained from rRNA 18S amplicon sequences.

phytoplankton species have nutritional requirements different than  $N : P = 16$ , and there are several “non-Redfield” processes in the aquatic ecosystem which may alter the  $N : P$  ratio, regardless of any nutrient limitation (Arrigo, 2005; Geider and La Roche, 2002; Moore et al., 2013).

The integrated chl  $a$  content at the background, the anticyclone and the cyclonic stations exhibited overall low variability ( $\sim 18\text{--}21 \text{ mg chl } a \text{ m}^{-2}$ ), yet the integrated primary production in the cyclone was  $\sim 5$  times higher, resulting in a higher assimilation number. This high assimilation number indicates a better efficiency of carbon incorporation per chl  $a$  unit and thus a better algal physiological state in the cyclone relative to that of other stations considered. This is likely owing to the higher nutrient availability (i.e.,  $N$  and  $P$ ) in the cyclone relative to the other more oligotrophic sites sampled (Table 1). It may also suggest different community compositions and cell sizes.

The overall low PP outside the cyclone (Fig. 3f, Table 1) is in accordance with another low-nutrient low-chl  $a$  (LNLC) system (Falkowski et al., 2003; Lomas et al., 2013) and aligned with the threshold limit of oligotrophic oceans:  $< 100 \text{ mg C m}^{-2} \text{ d}^{-1}$  (Koblentz-Mishke et al., 1970). Low PP

may be driven by several factors such as nutrient availability (Kress et al., 2005), light levels (Dishon et al., 2012; Sathyendranath and Platt, 2007; Stambler, 2012), viral infection (Guixa-Boixereu et al., 1999b, a) and top-down grazing by zooplankton (Griffin and Rippingale, 2001; Olli et al., 2007; Rakhesh et al., 2008). We surmise that the overall low PP was mainly driven by the  $N$  and  $P$  standing stocks in the photic layer, including the cyclone (Table 1). This is because light levels were similar at all stations and therefore unlikely to affect the daily PP rates between sites. Moreover, viral-induced mortality was shown to be less important than mortality due to grazing by protists in the SEMS as has been shown in unamended eastern Mediterranean surface water in mesocosms (Tsiola et al., 2017). By contrast, the grazing impact on phytoplankton was significantly higher in the cyclone compared to the other more oligotrophic sites ( $\sim 200\%$  vs.  $\sim 40\%$ – $100\%$ , respectively, Table 1). Despite the potentially high grazing pressure in the cyclone, higher phytoplankton biomass and PP were measured at this upwelling site. These differences between sites are likely attributed to the different phytoplankton growth rates, as phytoplankton’s doubling time at the cyclone was  $\sim 3$  d, while  $5\text{--}10$  d was estimated at the anticyclone and background stations. These doubling time estimates are in the same order as reported in other marine environments, ranging from  $\sim 1$  d (reviewed in Laws 2013) to 10 d (Dyhrman et al., 2012), and are in agreement with recent estimates from the central and western Mediterranean Sea (Marañón et al., 2021). We note that doubling time estimates have many caveats, mostly because some phytoplankton or bacteria comprise an unknown fraction of the POC pool, and it is a methodological challenge to separate them from all other particles in the water (Laws, 2013). Moreover, the grazing impact on PP calculated from mesozooplankton biomass alone may lead to an overestimation of the top-down impact on autotrophic microbial populations (Feliú et al., 2020). Therefore, it is likely that we overestimated the grazing impacts on PP, which exceeded  $100\%$  in the cyclone (Table 1). Some mesozooplankton species can simultaneously graze both phytoplankton and heterotrophic prey (i.e., heterotrophic dinoflagellates and ciliates, Dolan et al., 2002; Sherr and Sherr, 2007). Such a “multivorous” feeding strategy may explain the  $> 100\%$  mesozooplankton grazing impact on PP in the cyclone (Gasol et al., 1997). Moreover, the high estimated contribution of  $N$  and  $P$  by zooplankton to the PP by excretion in the cyclone ( $61\%$ – $85\%$ , Table 1) suggests rapid nutrient recycling that fuels the high production at this site. By contrast, at the anticyclone and background stations a lower  $N$  and  $P$  excretion by zooplankton was estimated (Table 1), therefore supporting only a minor part of the PP.

## 4.2 Heterotrophic bacterial abundance and production in anticyclonic and cyclonic waters of the SEMS

Prokaryotic microorganisms are important components of the marine food web, playing a pivotal role in many biogeochemical cycles (e.g., Kirchman, 2012). In warm and oligotrophic environments, such as the SEMS, heterotrophic bacterial metabolism is often equal to or even higher than autotrophic activity (Luna et al., 2012; Pulido-Villena et al., 2012; Rahav et al., 2019). Our results show that while the abundance of heterotrophs was overall similar in the cyclone and anticyclone, their cell-specific activity was nearly 3-fold higher in the nutrient-richer cyclone (Table 1). Given that average bacteria contain 14 fgC per cell (Gundersen et al., 2002), our estimate of bacterial cell-specific activity suggests that heterotroph doubling time in the cyclone is  $\sim 2$  times faster than at the less productive anticyclone and background stations (Table 1). The differences in cell-specific activity and corresponding doubling time between sites are likely supported by the supplementation of limiting nutrients for heterotrophic bacteria. Previous studies showed that P and/or dissolved organic carbon (DOC) are the limiting factors for heterotrophic microbial activity in the SEMS (Pitta et al., 2017; Rahav et al., 2019, 2021). We hypothesize that in the cyclone heterotrophic bacteria are likely DOC- rather than P-limited since the  $\text{PO}_4^{3+}$  concentrations at this location were  $\sim 3$ -fold higher than in the other locations (Table 1). The high mesozooplankton excretion in the cyclone may add DOC and inorganic nutrients, which could partly fulfill the metabolic requirements of the heterotrophic bacteria. By contrast, at the background and anticyclone stations heterotrophic prokaryotes were likely P-limited, as previously demonstrated in an onboard microcosm experiments (Rahav et al., 2021; Zohary et al., 2005) and using indirect N : P stoichiometric mass balance calculations (Krom et al., 2005).

The ratio between BP and PP is commonly used as an indicator for the carbon flux derived from photosynthesis channeled through the microbial heterotrophic food web (Cole et al., 1988). The higher the ratio, the lower the amount of carbon available for export through herbivorous food webs. Here, the BP rates were 2 times higher than PP in the LNLC anticyclone (Table 1), suggesting that microbial heterotrophs outcompeted phytoplankton for most of the available nutrients. The equal BP and PP at the background and the cyclone stations demonstrate an imbalanced microbial metabolism, highlighting the importance of heterotrophy in SEMS. Previous studies from the anticyclonic Cyprus Eddy (Thingstad et al., 2005) and throughout the Mediterranean Sea (Rahav et al., 2021) suggested that heterotrophic bacteria may outcompete phytoplankton or diazotrophs for  $\text{PO}_4^{3+}$ . This is in contrast to most oceanic regimes, in which  $\text{BP} : \text{PP} < 1$  in the photic layer (e.g., Lomas et al., 2013). We note that some studies suggest that a net heterotrophy in a given system is biased due to an underestimate of PP and/or an overestimate of respiration rate. We currently cannot refute nor re-

inforce this issue, as we did not measure respiration rates. Community respiration rate measurements, although technically challenging, are needed, especially in light of the future climate-change predictions stating the oceans will become more heterotrophic (Duarte et al., 2013).

The slope of the log–log linear regressions for BA (as biomass) and BP (a proxy of resource availability) suggest that bacterioplankton were bottom–up regulated in the anticyclone and top–down regulated in the cyclone (Billen et al., 1990; Ducklow, 1992; Pulido-Villena et al., 2012), in agreement with the estimated growth rates calculated above (Sect. 4.2). These values concur with other studies from Mediterranean offshore water where the log–log regression of BA vs. BP is usually  $\sim 0.40$  (Ducklow, 1992; Mével et al., 2008; Zohary and Robarts, 1998). Top–down and bottom–up factors are constantly changing in oligotrophic environments where organic-matter flux is sporadic rather than continuous and where PP and grazing pressure may vary greatly on a temporal scale (Pulido-Villena et al., 2012). Understanding the feedback mechanisms controlling heterotrophic bacterial abundance and production in LNLC environments is of great ecological importance, especially in areas such as the Mediterranean Sea where the water column is rapidly warming and thus heterotrophic metabolism is likely to be more dominant (Luna et al., 2012; Rahav et al., 2019).

## 4.3 Zooplankton biomass, estimated carbon and nutrient demand

Our results show that zooplankton biomass was 1 order of magnitude higher in the more productive cyclone than in the anticyclone and background stations. This is in line with previous studies (Goldthwait and Steinberg, 2008; Landry et al., 2008b; Liu et al., 2020; Riandey et al., 2005; including the Levantine Basin Mazzocchi et al., 1997; Pancucci-Papadopoulou et al., 1992), which showed that higher productivity (either as PP or chl *a* levels) in cyclonic eddies leads to higher zooplankton biomass. Zooplankton biomass reflected the higher PP in the photic layer rather than the standing stock of the primary producers, possibly due to the higher estimated grazing impact on phytoplankton stock at the cyclone vs. the anticyclone and background stations (Table 1). A recent study from the central and western Mediterranean Sea demonstrated that the nutrient diffusive fluxes across the nutricline contribute only a minor fraction of the phytoplankton N and P requirements in the deep photic layer (Marañón et al., 2021). This suggests that generally phytoplankton depend on regenerated nutrients for growth rather than their supply from the nutricline in the SEMS.

The estimated integrated contribution of zooplankton to carbon turnover and nutrient remineralization was markedly higher in the cyclone than at the anticyclone and background stations. Since the dietary needs of some zooplanktonic species diverge from the Redfield ratio (Arrigo, 2005; Geider and La Roche, 2002; Moore et al., 2013), our esti-

mates are based on the particulate C : N : P values reported from the Levantine Basin water (Pujo-Pay et al., 2011). The contribution of  $\text{PO}_4^{3+}$  by excretion of zooplankton to the estimated demand of phytoplankton was higher than their contribution of N ( $\sim 85\%$  vs.  $\sim 60\%$ , respectively). The fact that there is a markedly high excess of N relative to P in the photic layer of the cyclone (Table 1) implies that the P was consumed not only by phytoplankton. This further supports the “orthophosphate bypass theory” suggested by Thingstad et al. (2005), which showed that  $\text{PO}_4^{3+}$  can be rapidly transferred through the microbial food web to copepods, bypassing the phytoplankton compartment, via luxury consumption mechanisms that shift the stoichiometric composition of copepod prey.

In addition to the higher PP rates, the higher zooplankton concentrations in the cyclone may also be attributed to lower temperatures, potentially providing a thermal refuge for different larvae as shown by model simulations (Limer et al., 2020). Such a temporal or quasi-permanent shelter from detrimental environmental conditions can be especially important to the native biota in the rapidly warming Levantine Basin (Ozer et al., 2017). Furthermore, the warmer waters of anticyclonic eddies, arriving from the southeastern corner of the Levantine Basin (as in our case, Fig. S2), may carry thermophilic Indo-Pacific species and facilitate their introduction and spread throughout the SEMS. The potential role of cyclonic eddies as thermal refugia for native species and anticyclonic eddies as an introduction and dispersal vector for alien Indo-Pacific species should be investigated in future studies as cyclonic and anticyclonic features are likely to become more prominent in the future Mediterranean Sea (Siokou-Frangou et al., 2010).

#### 4.4 Diversity of bacterioplankton and planktonic protists

Multivariate analyses of bacterioplankton diversity suggest that at the DCM and 180 m depths, the bacterioplankton community at the cyclone station differed from that of the respective depths at the anticyclone and background stations (Fig. S10). These changes may be attributed to the depths of the nutricline, which vary between locations (Fig. 2), and/or selective grazing pressure caused by different zooplankton species with different nutrition preferences (see discussion below). The microbial communities at the cyclone station were more similar to those of the deeper depths at the anticyclone and background stations. For example, the DCM community of the cyclone resembled the community at 180 m depth of the anticyclone (Fig. S10). It has been shown that nutrient-poor anticyclonic gyres select for *Prochlorococcus* (Vaillancourt et al., 2003) and potentially for diazotrophs (Church et al., 2009; Fong et al., 2008; Rahav et al., 2013). Alongside the integrated cell counts (Table 1), diversity analyses suggest that *Prochlorococcus* is indeed most abundant in the anticyclone ( $\sim 8\%$  read abundance at the DCM) as op-

posed to  $\sim 5\%$ – $6\%$  in the control and cyclone’s DCM communities. We have, however, not identified cyanobacterial diazotrophs such as *Trichodesmium* and UCYN-A in any of our stations, in agreement with previous findings that showed uncoupling of PP and  $\text{N}_2$  fixations in the SEMS (Rahav et al., 2013). Apart from *Prochlorococcus*, ASVs of heterotrophic and mixotrophic lineages, such as SAR324, Flavobacteriales, Rhodospirillales, Punicespirillales, Opitiales, SAR86 and SAR11, were depleted at the cyclone’s DCM (DESeq2, adjusted  $p < 0.05$ ), implying a community-level shift driven by upwelling and downwelling processes. The actual drivers of these shifts (e.g., water mass movement, temperature, nutrient availability, interactions with another biota including phage predation) remain to be elucidated.

High N : P ratios were suggested to have a large effect on the diversity of micro-eukaryotes (e.g., Cercozoa, Ciliophora and Dinoflagellata), while pico- and nano-eukaryotes (e.g., dinoflagellates, Bacillariophyta, Chlorophyta and Haptophyta) are more adapted to the P-poor (and thus high N : P) conditions due to their high surface-to-volume ratio (Kruk and Segura, 2012). In agreement with this notation, we found that the Oligotrichia ciliates (Ciliophora) comprised  $\sim 9\%$  ASV read abundance in the cyclone DCM opposed to  $< 1\%$  at the anticyclone and background stations. These ciliates can feed on algae (as well as bacteria) and retain ingested chloroplasts (McManus et al., 2018) and thus potentially contribute to PP. However, we also identified a high read abundance of Radiolaria (RAD A, Retaria) at the anticyclone’s DCM ( $\sim 9\%$ , Fig. S5), indicating either that these organisms were indeed abundant or suggesting that radiolarians that often carry multiple nuclei (Suzuki et al., 2009) may introduce noise to the marker gene diversity results.

The potentially toxic dinoflagellate *Karlodinium* was most abundant at the anticyclone’s DCM (2.1%–2.6% of ASV reads) and least abundant at the cyclone station’s DCM (0.7% of ASV reads). A previous study suggested that the presence of this dinoflagellate may be related to P limitation, where it can switch from autotrophy to phagotrophy to take up nutrients from prey (Lin et al., 2016), providing it a competitive advantage. Indeed, the very low levels of  $\text{PO}_4^{3+}$  in the DCM of the anticyclone (below detection limit), opposed to the cyclone’s DCM ( $\sim 0.02 \mu\text{mol kg}^{-1}$ ), may explain the presence of this dinoflagellate and highlight that the different nutrient regimes may alter the diversity of protist communities in the SEMS.

Temperature is the main factor governing the distribution of planktonic protists in the SEMS (Santi et al., 2020). It is thus likely that the marked differences in the surface water temperature affect the diversity patterns of protists in warm and cold-core eddies. In the anticyclone, Syndiniales, which includes several known parasitic microbes (Guillou et al., 2008), were markedly enriched in surface waters (12 Syndiniales ASVs) relative to the other stations sampled. The relative abundance of these dominant parasites, which infect and kill other protists, such as dinoflagellates, cercozoans and

radiolarians as well as metazoans (Clarke et al., 2019), positively correlates with temperature (Anderson and Harvey, 2020). This is likely because temperature accelerates their metabolic rates, increasing infectivity and dinospore production (Anderson and Harvey, 2020; Coats and Park, 2002).

#### 4.5 Zooplankton diversity in anticyclonic vs. cyclonic waters at the SEMS

Cyclonic and anticyclonic eddies can entrain different zooplankton communities and biodiversity, distinctly different in their biogeographic origin from the adjacent waters (Hernández-León et al., 2001; Isla et al., 2004; Mackas et al., 2005; Pinca and Dallot, 1995; Riandey et al., 2005). In our study, we used meta-barcoding of mitochondrial (COI) and nuclear (18S) genes to assess the diversity of the mesozooplankton communities at the background, cyclone and anticyclone stations. We found that, although the background station had zooplankton biomass similar to that of the anticyclone, its community had high richness and diversity, comparable with that of the cyclone. Different and contrasting diversity patterns have been previously recorded in cyclonic vs. anticyclonic eddies relative to the surrounding waters. This includes reports on a higher diversity in cyclonic eddies (Matis et al., 2014; Pinca and Dallot, 1995), lower diversity in cyclonic eddies (Lavaniegos and Hereu, 2009), higher diversity in anticyclonic eddies (Dufois et al., 2016) and lower diversity in anticyclonic eddies as found in the majority of the studies (Holliday et al., 2011; Isari et al., 2011; Liu et al., 2020; Matis et al., 2014; Pinca and Dallot, 1997; Seguin et al., 1994). These contradicting patterns of diversity might be related to the difference in ages of the respective mesoscale features, as found in our case, or be related to the initial chemical characteristics of the respective environment (i.e., oligotrophic, mesotrophic or eutrophic). Low nutrient levels, as were measured in the anticyclone (Table 1), can promote the inter-specific competition for resources, favoring some species at the expense of others, thus decreasing species richness and evenness (Pinca and Dallot, 1997; Pitta et al., 2016; Seguin et al., 1994; Thingstad et al., 2005).

Copepods generally dominate mesozooplankton assemblages, both in terms of abundance and biomass and are important in the transfer of oceanic carbon and as a food source for higher trophic levels (Frangoulis et al., 2004). Because they are trophically diverse, the richness and diversity of copepods can reflect major changes in underlying patterns of production in the upper water column (Bonnet and Frid, 2004). In this study, copepod diversity presented a markedly large difference between the species-rich cyclone (44 species) and the species-poor anticyclone (6 species). Most of the copepod species in the anticyclone were small-body calanoids, e.g., *Clausocalanus* and *Calocalanus* species. Medium- and larger-size calanoid copepods, such as *Pleuromamma*, *Euchirella*, *Scolecithricella*, *Ctenocalanus*, *Nannocalanus* and *Mesocalanus*, were only present

in the cyclone and background stations. Similar diversity patterns were observed in the Liguro-Provençal Basin, cyclonic and anticyclonic gyres in the Ionian and Levantine seas, and the Black Sea (Pinca and Dallot, 1997; Siokou-Frangou et al., 1997). In contrast to calanoid copepods, the *Oncaea* species was present only in the cyclone; these cruising detritivores likely benefit from the relatively higher phytoplankton biomass and productivity (Fig. 3 and Table 1).

Cyclonic structures have been associated with favorable habitats for reproduction and larval recruitment of many fish species, entraining higher larval abundance and diversity (Bakun, 2010; Condie and Condie, 2016; Logerwell and Smith, 2001; Matis et al., 2014; Mullaney and Suthers, 2013). In this study, we found a higher diversity of fish larvae and eggs in the cyclone, mainly including *Engraulis encrasicolus* (the European anchovy). Upwelling regions in the Alboran Sea, the Gulf of Lion and the nearby Catalan Sea, the Adriatic Sea, and the north Aegean Sea are known as successful spawning grounds and areas of high productivity of small pelagic fish, mainly anchovy and sardine (Agostini and Bakun, 2002; Palomera et al., 2007; Stergiou et al., 1997). In the impoverished SEMS, the importance of cyclonic eddies as “high-productivity islands” for fish reproduction and recruitment might be high. Indeed, our finding suggests that cyclonic eddies may serve as reproduction hotspots and nursery grounds of anchovies.

Other taxonomic groups, specifically chaetognaths, polychaetes, cladocerans, and pelagic amphipods and decapods, exhibited higher richness in the cyclone compared to the anticyclone. An exception to the higher species diversity within the cyclone was the gastropods that showed higher diversity in the anticyclone station. A potential reason could be the thermophilic nature of many of the taxa identified in the anticyclone, including the larvae of a Red Sea Lessepsian invader, *Nerita sanguinolenta*. An adult individual of this species was recently recorded on the Israeli Mediterranean coast for the first time (Rabi et al., 2020). Mesoscale and sub-mesoscale structures can promote introductions of invasive species or recruitment of harmful species, such as the destructive crown-of-thorns starfish (Miller et al., 2015), the extremely venomous box jellyfish *Irukandji* (Gershwin et al., 2013) and a sea urchin overgrazing the kelp forests (Ling and Johnson, 2009). In the SEMS, anticyclonic eddies originate from the alongshore current in the southeastern corner of the basin, in the vicinity of the Suez Canal opening. We can therefore hypothesize that the higher temperatures in anticyclonic eddies and their southeastern origin might facilitate the introduction and spread of the warm-adapted invasive Red Sea species. This finding has important implications for conservation and management and should be followed by additional research to substantiate the connection between Lessepsian invasive species and hydrodynamic structures in the Mediterranean Sea. Moreover, more studies of mesoscale features through their lifetime are required to improve the predictions of future conditions and to model the productiv-



ity of the Mediterranean Sea and other LNLC regimes in light of global climate changes and the need to reduce the atmospheric carbon footprint.

**Data availability.** The data are presented in full in the main text or the Supplement. Genetic material was deposited in NCBI Sequence Read Archive BioProject PRJNA667077 (<https://www.ncbi.nlm.nih.gov/bioproject/?term=PRJNA667077>, Guy-Haim, 2020).

**Supplement.** The supplement related to this article is available online at: <https://doi.org/10.5194/os-18-693-2022-supplement>.

**Author contributions.** NB, TGH, MRB, AL, BH and ER conceptualized the study. IG, TO, TGH and AL were responsible for data curation. NB, TGH, MRB, RK, ARM, GSV, AL, and ER carried out the formal analysis. Project administration was carried out by AL and GSV. NB, TGH, RK, MRB, AL, IG, TO, BH and ER wrote the original draft.

**Competing interests.** The contact author has declared that neither they nor their co-authors have any competing interests.

**Disclaimer.** Publisher's note: Copernicus Publications remains neutral with regard to jurisdictional claims in published maps and institutional affiliations.

**Special issue statement.** This article is part of the special issue “Advances in interdisciplinary studies at multiple scales in the Mediterranean Sea”. It is not associated with a conference.

**Acknowledgements.** We would like to thank the R.V. *Bat-Galim* captains and crew for help at sea. The authors also thank Briac Le Vu, Evangelos Moschos and Alexandre Stegner for producing the AMEDA map and François Carlotti and Marc Pagano for their help with zooplankton rate calculations.

**Financial support.** This research has been supported by the Israel Science Foundation (grant no. 1666/18), the National Monitoring Program of Israel's Mediterranean waters, the Israel Science Foundation (grant no. 1666/18 to Ayah Lazar) and the Ministry of Science and Technology (MOST) (grant no. 3-17933 to Tamar Guy-Haim). Rainer Kiko received funding from the Deutsche Forschungsgemeinschaft as part of the Sonderforschungsbereich 754 “Climate–Biogeochemistry Interactions in the Tropical Ocean” and by a Make Our Planet Great Again grant of the French Agence Nationale de la Recherche under the “Programme d'Investissements d'Avenir”, reference ANR-19-MPGA-0012.

**Review statement.** This paper was edited by Vanessa Cardin and reviewed by Milena Menna and two anonymous referees.

## References

- Agostini, V. N. and Bakun, A.: “Ocean triads” in the Mediterranean Sea: Physical mechanisms potentially structuring reproductive habitat suitability (with example application to European anchovy, *Engraulis encrasicolus*), *Fish. Oceanogr.*, 11, 129–142, <https://doi.org/10.1046/j.1365-2419.2002.00201.x>, 2002.
- Alcaraz, M., Calbet, A., Estrada, M., Marrasé, C., Saiz, E., and Trepas, I.: Physical control of zooplankton communities in the Catalan Sea, *Prog. Oceanogr.*, 74, 294–312, <https://doi.org/10.1016/j.pocean.2007.04.003>, 2007.
- Allen, C. B., Kanda, J., and Laws, E. A.: New production and photosynthetic rates within and outside a cyclonic mesoscale eddy in the North Pacific subtropical gyre, *Deep-Res. Pt. I*, 43, 917–936, [https://doi.org/10.1016/0967-0637\(96\)00022-2](https://doi.org/10.1016/0967-0637(96)00022-2) 1996.
- Amaral-Zettler, L. A., McCliment, E. A., Ducklow, H. W., and Huse, S. M.: A method for studying protistan diversity using massively parallel sequencing of V9 hypervariable regions of small-subunit ribosomal RNA Genes, *PLoS One*, 4, 1–9, <https://doi.org/10.1371/journal.pone.0006372>, 2009.
- Andersen, K. S., Kirkegaard, R. H., Karst, S. M., and Albertsen, M.: ampvis2: an R package to analyse and visualise 16S rRNA amplicon data, *BioRxiv*, 10–11, <https://doi.org/10.1101/299537>, 2018.
- Anderson, S. R. and Harvey, E. L.: Temporal variability and ecological interactions of parasitic marine Symbionts in coastal protist communities, *mSphere*, 5, 1–16, <https://doi.org/10.1128/msphere.00209-20>, 2020.
- Andrade, J. M. and Estévez-Pérez, M. G.: Statistical comparison of the slopes of two regression lines: A tutorial, *Anal. Chim. Acta*, 838, 1–12, <https://doi.org/10.1016/j.aca.2014.04.057>, 2014.
- Ansotegui, A., Sarobe, A., María Trigueros, J., Urrutxurtu, I., and Orive, E.: Size distribution of algal pigments and phytoplankton assemblages in a coastal-estuarine environment: Contribution of small eukaryotic algae, *J. Plankton Res.*, 25, 341–355, <https://doi.org/10.1093/plankt/25.4.341>, 2003.
- Apprill, A., McNally, S., Parsons, R., and Weber, L.: Minor revision to V4 region SSU rRNA 806R gene primer greatly increases detection of SAR11 bacterioplankton, *Aquat. Microb. Ecol.*, 75, 129–137, <https://doi.org/10.3354/ame01753>, 2015.
- Arrigo, K.: Marine microorganisms and global nutrient cycles, *Nature*, 437, 349–355, 2005.
- Bakun, A.: Linking climate to population variability in marine ecosystems characterized by non-simple dynamics: Conceptual templates and schematic constructs, *J. Marine Syst.*, 79, 361–373, <https://doi.org/10.1016/j.jmarsys.2008.12.008>, 2010.
- Berman-Frank, I. and Rahav, E.: Nitrogen fixation as a source for new production in the Mediterranean Sea: A review, in: *Life in the Mediterranean Sea: A Look at Habitat Changes*, edited by: Stambler, N., Nova Science Publishers, NY, 199–226, ISBN 978-1-61209-644-5, 2012.
- Berman, T., Townsend, D., and Elsayed, S.: Optical transparency, chlorophyll and primary productivity in the eastern Mediterranean near the Israeli coast, *Oceanol. Acta*, 7, 367–372, 1984.

- Billen, G., Servais, P., and Becquevort, S.: Dynamics of bacterioplankton in oligotrophic and eutrophic aquatic environments: bottom-up or top-down control?, *Hydrobiologia*, 207, 37–42, <https://doi.org/10.1007/BF00041438>, 1990.
- Bolyen, E., Rideout, J. R., Dillon, M. R., Bokulich, N. A., Abnet, C. C., Al-Ghalith, G. A., Alexander, H., Alm, E. J., Arumugam, M., Asnicar, F., Bai, Y., Bisanz, J. E., Bittinger, K., Brejnrod, A., Brislawn, C. J., Brown, C. T., Callahan, B. J., Caraballo-Rodríguez, A. M., Chase, J., Cope, E. K., Da Silva, R., Diener, C., Dorrestein, P. C., Douglas, G. M., Durall, D. M., Duvallet, C., Edwardson, C. F., Ernst, M., Estaki, M., Fouquier, J., Gauglitz, J. M., Gibbons, S. M., Gibson, D. L., Gonzalez, A., Gorlick, K., Guo, J., Hillmann, B., Holmes, S., Holste, H., Huttenhower, C., Huttley, G. A., Janssen, S., Jarmusch, A. K., Jiang, L., Kaehler, B. D., Kang, K. Bin, Keefe, C. R., Keim, P., Kelley, S. T., Knights, D., Koester, I., Kosciolk, T., Kreps, J., Langille, M. G. I., Lee, J., Ley, R., Liu, Y. X., Loftfield, E., Lozupone, C., Maher, M., Marotz, C., Martin, B. D., McDonald, D., McIver, L. J., Melnik, A. V., Metcalf, J. L., Morgan, S. C., Morton, J. T., Naimey, A. T., Navas-Molina, J. A., Nothias, L. F., Orchanian, S. B., Pearson, T., Peoples, S. L., Petras, D., Preuss, M. L., Pruesse, E., Rasmussen, L. B., Rivers, A., Robeson, M. S., Rosenthal, P., Segata, N., Shaffer, M., Shiffer, A., Sinha, R., Song, S. J., Spear, J. R., Swafford, A. D., Thompson, L. R., Torres, P. J., Trinh, P., Tripathi, A., Turnbaugh, P. J., Ul-Hasan, S., van der Hoof, J. J. J., Vargas, F., Vázquez-Baeza, Y., Vogtmann, E., von Hippel, M., et al.: Reproducible, interactive, scalable and extensible microbiome data science using QIIME 2, *Nat. Biotechnol.*, 37, 852–857, <https://doi.org/10.1038/s41587-019-0209-9>, 2019.
- Bonnet, D. and Frid, C.: Seven copepod species considered as indicators of water-mass influence and changes: Results from a Northumberland coastal station, *ICES J. Mar. Sci.*, 61, 485–491, <https://doi.org/10.1016/j.icesjms.2004.03.005>, 2004.
- Calbet, A., Alcaraz, M., Saiz, E., Estrada, M., and Trepát, I.: Planktonic herbivorous food webs in the catalan sea (NW Mediterranean): Temporal variability and comparison of indices of phyto-zooplankton coupling based on state variables and rate processes, *J. Plankton Res.*, 18, 2329–2347, <https://doi.org/10.1093/plankt/18.12.2329>, 1996.
- Callahan, B. J., McMurdie, P. J., Rosen, M. J., Han, A. W., Johnson, A. J. A., and Holmes, S. P.: DADA2: High-resolution sample inference from Illumina amplicon data, *Nat. Methods*, 13, 581–583, <https://doi.org/10.1038/nmeth.3869>, 2016.
- Campbell, L. and Vault, D.: Photosynthetic picoplankton community structure in the subtropical North Pacific Ocean near Hawaii (station ALOHA), *Deep-Res. Pt. I*, 40, 2043–2060, [https://doi.org/10.1016/0967-0637\(93\)90044-4](https://doi.org/10.1016/0967-0637(93)90044-4), 1993.
- Christaki, U.: Nanoflagellate predation on auto- and heterotrophic picoplankton in the oligotrophic Mediterranean Sea, *J. Plankton Res.*, 23, 1297–1310, <https://doi.org/10.1093/plankt/23.11.1297>, 2001.
- Christaki, U., Van Wambeke, F., Lefevre, D., Lagaria, A., Prieur, L., Pujo-Pay, M., Grattepanche, J.-D., Colombet, J., Psarra, S., Dolan, J. R., Sime-Ngando, T., Conan, P., Weinbauer, M. G., and Moutin, T.: Microbial food webs and metabolic state across oligotrophic waters of the Mediterranean Sea during summer, *Biogeosciences*, 8, 1839–1852, <https://doi.org/10.5194/bg-8-1839-2011>, 2011.
- Christou, E. D.: Interannual variability of copepods in a Mediterranean coastal area (Saronikos Gulf, Aegean Sea), *J. Marine Syst.*, 15, 523–532, [https://doi.org/10.1016/S0924-7963\(97\)00080-8](https://doi.org/10.1016/S0924-7963(97)00080-8), 1998.
- Church, M. J., Mahaffey, C., Letelier, R. M., Lukas, R., Zehr, J. P., and Karl, D. M.: Physical forcing of nitrogen fixation and diazotroph community structure in the North Pacific subtropical gyre, *Global Biogeochem. Cy.*, 23, GB2020, <https://doi.org/10.1029/2008GB003418>, 2009.
- Clarke, L. J., Bestley, S., Bissett, A., and Deagle, B. E.: A globally distributed *Syndiniales* parasite dominates the Southern Ocean micro-eukaryote community near the sea-ice edge, *ISME J.*, 13, 734–737, <https://doi.org/10.1038/s41396-018-0306-7>, 2019.
- Coats, D. W. and Park, M. G.: Parasitism of photosynthetic dinoflagellates by three strains of *Amoebophrya* (Dinophyta): Parasite survival, infectivity, generation time, and host specificity, *J. Phycol.*, 38, 520–528, <https://doi.org/10.1046/j.1529-8817.2002.01200.x>, 2002.
- Cole, J., Findlay, S., and Pace, M.: Bacterial production in fresh and saltwater ecosystems – A cross-system overview, *Mar. Ecol. Prog. Ser.*, 43, 1–10, 1988.
- Colgan, D. J., Hutchings, P. A., and Braune, M.: A multigene framework for polychaete phylogenetic studies, *Org. Divers. Evol.*, 6, 220–235, <https://doi.org/10.1016/j.ode.2005.11.002>, 2006.
- Condie, S. and Condie, R.: Retention of plankton within ocean eddies, *Global Ecol. Biogeogr.*, 25, 1264–1277, <https://doi.org/10.1111/geb.12485>, 2016.
- Dishon, G., Dubinsky, Z., Caras, T., Rahav, E., Bar-Zeev, E., Tzuber, Y., and Iluz, D.: Optical habitats of ultraphytoplankton groups in the Gulf of Eilat (Aqaba), Northern Red Sea, *Int. J. Remote Sens.*, 33, 2683–2705, <https://doi.org/10.1080/01431161.2011.619209>, 2012.
- Djaoudi, K., Van Wambeke, F., Coppola, L., D’Ortenzio, F., Helias-Nunige, S., Raimbault, P., Taillandier, V., Testor, P., Wagener, T., and Pulido-Villena, E.: Sensitive Determination of the Dissolved Phosphate Pool for an Improved Resolution of Its Vertical Variability in the Surface Layer: New Views in the P-Depleted Mediterranean Sea, *Front. Mar. Sci.*, 5, 1–11, <https://doi.org/10.3389/fmars.2018.00234>, 2018.
- Dolan, J. R. and Marrasé, C.: Planktonic ciliate distribution relative to a deep chlorophyll maximum: Catalan Sea, N. W. Mediterranean, June 1993, *Deep-Res. Pt. I*, 42, 1965–1987, [https://doi.org/10.1016/0967-0637\(95\)00092-5](https://doi.org/10.1016/0967-0637(95)00092-5), 1995.
- Dolan, J. R., Claustre, H., Carlotti, F., Plounevez, S., and Moutin, T.: Microzooplankton diversity: Relationships of tintinnid ciliates with resources, competitors and predators from the Atlantic Coast of Morocco to the Eastern Mediterranean, *Deep-Res. Pt. I Oceanogr. Res. Pap.*, 49, 1217–1232, [https://doi.org/10.1016/S0967-0637\(02\)00021-3](https://doi.org/10.1016/S0967-0637(02)00021-3), 2002.
- Duarte, C. M., Duarte, C. M., Regaudie-de-gioux, A., and Agust, S.: The oligotrophic ocean is heterotrophic, *Ann. Rev. Mar. Sci.*, 5, 551–569, <https://doi.org/10.1146/annurev-marine-121211-172337>, 2013.
- Ducklow, H. W. and Carlson, C. A.: Oceanic bacterial production, in: *Advances in Microbial Ecology*, edited by: Marshall, K. C., Springer, Boston, MA, 113–181, [https://doi.org/10.1007/978-1-4684-7609-5\\_3](https://doi.org/10.1007/978-1-4684-7609-5_3), 1992.
- Dufois, F., Hardman-Mountford, N. J., Greenwood, J., Richardson, A. J., Feng, M., and Matear, R. J.: Anticyclonic ed-

- dies are more productive than cyclonic eddies in subtropical gyres because of winter mixing, *Sci. Adv.*, 2, 1–7, <https://doi.org/10.1126/sciadv.1600282>, 2016.
- Dyhrman, S. T., Jenkins, B. D., Rynearson, T. A., Saito, M. A., Mercier, M. L., Alexander, H., Whitney, L. P., Drzewianowski, A., Bulygin, V. V., Bertrand, E. M., Wu, Z., Benitez-nelson, C., and Heithoff, A.: The Transcriptome and Proteome of the Diatom *Thalassiosira pseudonana* Reveal a Diverse Phosphorus Stress Response, *PLoS One*, 7, e33768, <https://doi.org/10.1371/journal.pone.0033768>, 2012.
- Efrati, S., Lehahn, Y., Rahav, E., Kress, N., Herut, B., Gertman, I., Goldman, R., Ozer, T., Lazar, M., and Heifetz, E.: Intrusion of coastal waters into the pelagic eastern Mediterranean: in situ and satellite-based characterization, *Biogeosciences*, 10, 3349–3357, <https://doi.org/10.5194/bg-10-3349-2013>, 2013.
- Falkowski, P. G., Ziemann, D., Kolber, Z., and Bienfang, P. K.: Role of eddy pumping in enhancing primary production in the ocean, *Nature*, 352, 55–58, <https://doi.org/10.1038/352055a0>, 1991.
- Falkowski, P. G., Laws, E. A., Barber, R. T., and Murray, J. W.: Phytoplankton and Their Role in Primary, New, and Export Production, in *Ocean Biogeochemistry*, pp. 99–121, Springer Berlin Heidelberg, Berlin, Heidelberg, 2003.
- Feliú, G., Pagano, M., Hidalgo, P., and Carlotti, F.: Structure and function of epipelagic mesozooplankton and their response to dust deposition events during the spring PEACETIME cruise in the Mediterranean Sea, *Biogeosciences*, 17, 5417–5441, <https://doi.org/10.5194/bg-17-5417-2020>, 2020.
- Fong, A. A., Karl, D. M., Lukas, R., Letelier, R. M., Zehr, J. P., and Church, M. J.: Nitrogen fixation in an anticyclonic eddy in the oligotrophic North Pac, *ISME J.*, 2, 663–676, <https://doi.org/10.1038/ismej.2008.22>, 2008.
- Frangoulis, C., Christou, E. D., and Hecq, J. H.: Comparison of marine copepod outfluxes: Nature, rate, fate and role in the carbon and nitrogen cycles., 2004.
- Gasol, J. M., Del Giorgio, P. A., and Duarte, C. M.: Biomass distribution in marine planktonic communities, *Limnol. Oceanogr.*, 42, 1353–1363, <https://doi.org/10.4319/lo.1997.42.6.1353>, 1997.
- Gaube, P., McGillicuddy, D. J., Chelton, D. B., Behrenfeld, M. J., and Strutton, P. G.: Regional variations in the influence of mesoscale eddies on near-surface chlorophyll, *J. Geophys. Res. Ocean.*, 119, 8195–8220, <https://doi.org/10.1002/2014JC010111>, 2014.
- Geider, R. J. and La Roche, J.: Redfield revisited: Variability of C : N : P in marine microalgae and its biochemical basis, *Eur. J. Phycol.*, 37, 1–17, <https://doi.org/10.1017/S0967026201003456>, 2002.
- Gershwin, L. ann, Richardson, A. J., Winkel, K. D., Fenner, P. J., Lippmann, J., Hore, R., Avila-Soria, G., Brewer, D., Kloser, R. J., Steven, A., and Condie, S.: *Biology and Ecology of Irukandji Jellyfish (Cnidaria: Cubozoa)*, 1st ed., Elsevier Ltd., 2013.
- Goldthwait, S. A. and Steinberg, D. K.: Elevated biomass of mesozooplankton and enhanced fecal pellet flux in cyclonic and mode-water eddies in the Sargasso Sea, *Deep-Res. Pt. II*, 55, 1360–1377, <https://doi.org/10.1016/j.dsr2.2008.01.003>, 2008.
- Griffin, S. L. and Rippingale, R. J.: Zooplankton grazing dynamics: Top-down control of phytoplankton and its relationship to an estuarine habitat, *Hydrol. Process.*, 15, 2453–2464, <https://doi.org/10.1002/hyp.293>, 2001.
- Groom, S., Herut, B., Brenner, S., Zodiatis, G., Psarra, S., Kress, N., Krom, M. D., Law, C. S., and Drakopoulos, P.: Satellite-derived spatial and temporal biological variability in the Cyprus Eddy, *Deep-Res. Pt. II*, 52, 2990–3010, <https://doi.org/10.1016/j.dsr2.2005.08.019>, 2005.
- Guillou, L., Viprey, M., Chambouvet, A., Welsh, R. M., Kirkham, A. R., Massana, R., Scanlan, D. J., and Worden, A. Z.: Widespread occurrence and genetic diversity of marine parasitoids belonging to *Syndiniales (Alveolata)*, *Environ. Microb.*, 10, 3349–3365, <https://doi.org/10.1111/j.1462-2920.2008.01731.x>, 2008.
- Guixa-Boixereu, N., Vaque, D., Gasol, J. M., and Pedrós-Alió, C.: Distribution of viruses and their potential effect on bacterioplankton in an oligotrophic marine system, *Aquat. Microb. Ecol.*, 19, 205–213, <https://doi.org/10.3354/ame019205>, 1999a.
- Guixa-Boixereu, N., Lysnes, K., Guixa-boixereu, R. I. A., and Lysnes, K.: Viral lysis and bacterivory during a phytoplankton bloom in a coastal water microcosm, *Appl. Environ. Microb.*, 65, 1949–1958, 1999b.
- Gundersen, K., Heldal, M., Norland, S., Purdie, D. A., and Knap, A. H.: Elemental C, N, and P cell content of individual bacteria collected at the Bermuda Atlantic Time-series Study (BATS) site, *Limnol. Oceanogr.*, 47, 1525–1530, <https://doi.org/10.4319/lo.2002.47.5.1525>, 2002.
- Guy-Haim, T.: Mixed zooplankton net samples from cyclonic eddy, anti-cyclonic eddy and background stations in the Israeli Mediterranean Sea, in: NCBI BioProject no. 667077, <https://www.ncbi.nlm.nih.gov/bioproject/?term=PRJNA667077> (last access: May 2022), 2020.
- Harris, R., Wiebe, P., Lenz, J., Skjoldal, H., and Huntley, M.: *ICES Zooplankton Methodology Manual*, 1st edn., edited by: Harris, R., Wiebe, P., Lenz, J., Skjoldal, H., and Huntley, M., Academic Press, San Diego, ISBN 9780123276452, 2000.
- Hazan, O., Silverman, J., Sisma-Ventura, G., Ozer, T., Gertman, I., Shoham-Frider, E., Kress, N., and Rahav, E.: Mesopelagic prokaryotes alter surface phytoplankton production during simulated deep mixing experiments in Eastern Mediterranean Sea waters, *Front. Mar. Sci.*, 5, <https://doi.org/10.3389/fmars.2018.00001>, 2018.
- Heller, P., Casaletto, J., Ruiz, G., and Geller, J.: Data Descriptor: A database of metazoan cytochrome c oxidase subunit I gene sequences derived from GenBank with CO-ARBITRATOR, *Sci. Data*, 5, 1–7, <https://doi.org/10.1038/sdata.2018.156>, 2018.
- Hernández-León, S., Almeida, C., Gómez, M., Torres, S., Montero, I., and Portillo-Hahnefeld, A.: Zooplankton biomass and indices of feeding and metabolism in island-generated eddies around Gran Canaria, *J. Marine Syst.*, 30, 51–66, [https://doi.org/10.1016/S0924-7963\(01\)00037-9](https://doi.org/10.1016/S0924-7963(01)00037-9), 2001.
- Herut, B., Collier, R., and Krom, M. D.: The role of dust in supplying nitrogen and phosphorus to the south-east Mediterranean, *Limnol. Oceanogr.*, 47, 870–878, <https://doi.org/10.4319/lo.2002.47.3.0870>, 2002.
- Herut, B., Zohary, T., Krom, M. D. D., Mantoura, R. F. C., Pitta, P., Psarra, S., Rassoulzadegan, F., Tanaka, T., and Frede Thingstad, T.: Response of East Mediterranean surface water to Saharan dust: On-board microcosm experiment and field observations, *Deep-Res. Pt. II*, 52, 3024–3040, <https://doi.org/10.1016/j.dsr2.2005.09.003>, 2005.

- Holliday, D., Beckley, L. E., and Olivar, M. P.: Incorporation of larval fishes into a developing anti-cyclonic eddy of the Leeuwin Current off south-western Australia, *J. Plankton Res.*, 33, 1696–1708, <https://doi.org/10.1093/plankt/fbr064>, 2011.
- Houlbrèque, F., Delesalle, B., Blanchot, J., Montel, Y., and Ferrier-Pagès, C.: Picoplankton removal by the coral reef community of La Prévoyante, Mayotte Island, *Aquat. Microb. Ecol.*, 44, 59–70, <https://doi.org/10.3354/ame044059>, 2006.
- Huggett, J. A.: Mesoscale distribution and community composition of zooplankton in the Mozambique Channel, *Deep-Res. Pt. II*, 100, 119–135, <https://doi.org/10.1016/j.dsr2.2013.10.021>, 2014.
- Ignatiades, L., Psarra, S., Zervakis, V., Pagou, K., Souvermezoglou, E., Assimakopoulou, G., and Gotsis-Skretas, O.: Phytoplankton size-based dynamics in the Aegean Sea (Eastern Mediterranean), *J. Marine Syst.*, 36, 11–28, [https://doi.org/10.1016/S0924-7963\(02\)00132-X](https://doi.org/10.1016/S0924-7963(02)00132-X), 2002.
- Ikeda, T.: Metabolic rates of epipelagic marine zooplankton as a function of body mass and temperature, *Mar. Biol.*, 85, 1–11, <https://doi.org/10.1007/BF00396409>, 1985.
- Ikeda, T., Torres, J. J., Hernandez-Leon, S., and Geiger, S. P.: Metabolism, in: ICES zooplankton methodology manual, edited by: Harris, R., pp. 455–532, Academic Press, London, 2000.
- Ioannou, A., Stegner, A., Tuel, A., LeVu, B., Dumas, F., and Speich, S.: Cyclostrophic Corrections of AVISO/DUACS Surface Velocities and Its Application to Mesoscale Eddies in the Mediterranean Sea, *J. Geophys. Res.-Oceans*, 124, 8913–8932, <https://doi.org/10.1029/2019JC015031>, 2019.
- Isari, S., Somarakis, S., Christou, E. D., and Fragopoulou, N.: Summer mesozooplankton assemblages in the north-eastern Aegean Sea: The influence of Black Sea water and an associated anticyclonic eddy, *J. Mar. Biol. Assoc. UK*, 91, 51–63, <https://doi.org/10.1017/S0025315410000123>, 2011.
- Isla, J. A., Ceballos, S., Huskin, I., Anadón, R., and Álvarez-Marqués, F.: Mesozooplankton distribution, metabolism and grazing in an anticyclonic slope water oceanic eddy (SWODDY) in the Bay of Biscay, *Mar. Biol.*, 145, 1201–1212, <https://doi.org/10.1007/s00227-004-1408-5>, 2004.
- Jeffrey, S. W., Mantoura, R. F. C., and Wright, S. W. (Eds.): *Phytoplankton pigments in oceanography: guidelines to modern methods*, 1st edn., UNESCO, Paris, 1997.
- Kirchman, D. L. (Ed.): *Processes in microbial ecology*, 1st edn., Oxford University Press, Oxford, 2012.
- Koblentz-Mishke, O. J., Volrovinsky, V. V., and Kabanova, J. G.: Plankton primary production of the world ocean, in: *Scientific exploration of the South Pacific*, edited by: Wooster, W. S., National Academy of Sciences, Washington, DC, pp. 183–193, 1970.
- Koppelman, R., Böttger-Schnack, R., Möbius, J., and Weikert, H.: Trophic relationships of zooplankton in the eastern Mediterranean based on stable isotope measurements, *J. Plankton Res.*, 31, 669–686, <https://doi.org/10.1093/plankt/fbp013>, 2009.
- Kress, N., Frede Thingstad, T., Pitta, P., Psarra, S., Tanaka, T., Zohary, T., Groom, S., Herut, B., Fauzi, R., Polychronaki, T., Rasoulzadegan, F., and Spyres, G.: Effect of P and N addition to oligotrophic Eastern Mediterranean waters influenced by near-shore waters: A microcosm experiment, *Deep-Res. Pt. II*, 52, 3054–3073, <https://doi.org/10.1016/j.dsr2.2005.08.013>, 2005.
- Kress, N., Gertman, I., and Herut, B.: Temporal evolution of physical and chemical characteristics of the water column in the Easternmost Levantine Basin (Eastern Mediterranean Sea) from 2002 to 2010, *J. Marine Syst.*, 135, 6–13, <https://doi.org/10.1016/j.jmarsys.2013.11.016>, 2014.
- Krom, M. D., Woodward, E. M. S., Herut, B., Kress, N., Carbo, P., Mantoura, R. F. C., Spyres, G., Thingsted, T. F., Wassmann, P., Wexels-Riser, C., Kitidis, V., Law, C., and Zodiatis, G.: Nutrient cycling in the south east Levantine basin of the eastern Mediterranean: Results from a phosphorus starved system, *Deep-Res. Pt. II*, 52, 2879–2896, <https://doi.org/10.1016/j.dsr2.2005.08.009>, 2005.
- Kruk, C. and Segura, A. M.: The habitat template of phytoplankton morphology-based functional groups, *Hydrobiologia*, 698, 191–202, <https://doi.org/10.1007/s10750-012-1072-6>, 2012.
- Landry, M. R., Brown, S. L., Rii, Y. M., Selph, K. E., Bidigare, R. R., Yang, E. J., and Simmons, M. P.: Depth-stratified phytoplankton dynamics in Cyclone Opal, a subtropical mesoscale eddy, *Deep-Res. Pt. II*, 55, 1348–1359, <https://doi.org/10.1016/j.dsr2.2008.02.001>, 2008a.
- Landry, M. R., Decima, M., Simmons, M. P., Hannides, C. C. S., and Daniels, E.: Mesozooplankton biomass and grazing responses to Cyclone Opal, a subtropical mesoscale eddy, *Deep-Res. Pt. II*, 55, 1378–1388, <https://doi.org/10.1016/j.dsr2.2008.01.005>, 2008b.
- Lavaniegos, B. E. and Hereu, C. M.: Seasonal variation in hyperiid amphipod abundance and diversity and influence of mesoscale structures off Baja California, *Mar. Ecol. Prog. Ser.*, 394, 137–152, <https://doi.org/10.3354/meps08285>, 2009.
- Laws, E. A.: Evaluation of In Situ Phytoplankton Growth Rates: A Synthesis of Data from Varied Approaches, *Annu. Rev. Mar. Sci.*, 5, 247–268, <https://doi.org/10.1146/annurev-marine-121211-172258>, 2013.
- Le Vu, B., Stegner, A., and Arsouze, T.: Angular momentum eddy detection and tracking algorithm (AMEDA) and its application to coastal eddy formation, *J. Atmos. Ocean. Tech.*, 35, 739–762, <https://doi.org/10.1175/JTECH-D-17-0010.1>, 2018.
- Limer, B. D., Bloomberg, J., and Holstein, D. M.: The Influence of Eddies on Coral Larval Retention in the Flower Garden Banks, *Front. Mar. Sci.*, 7, 1–16, <https://doi.org/10.3389/fmars.2020.00372>, 2020.
- Lin, S., Litaker, R. W., and Sunda, W. G.: Phosphorus physiological ecology and molecular mechanisms in marine phytoplankton, *J. Phycol.*, 52, 10–36, <https://doi.org/10.1111/jpy.12365>, 2016.
- Ling, S. D. and Johnson, C. R.: Population dynamics of an ecologically important range-extender: Kelp beds versus sea urchin barrens, *Mar. Ecol. Prog. Ser.*, 374, 113–125, <https://doi.org/10.3354/meps07729>, 2009.
- Liu, H., Zhu, M., Guo, S., Zhao, X., and Sun, X.: Effects of an anticyclonic eddy on the distribution and community structure of zooplankton in the South China Sea northern slope, *J. Marine Syst.*, 205, 103311, <https://doi.org/10.1016/j.jmarsys.2020.103311>, 2020.
- Logerwell, E. A. and Smith, P. E.: Mesoscale eddies and survival of late stage Pacific sardine (*Sardinops sagax*) larvae, *Fish. Oceanogr.*, 10, 13–25, <https://doi.org/10.1046/j.1365-2419.2001.00152.x>, 2001.
- Lomas, M. W., Bates, N. R., Johnson, R. J., Knap, A. H., Steinberg, D. K., and Carlson, C. A.: Two decades and counting: 24-years of sustained open ocean biogeochemical mea-

- surements in the Sargasso Sea, *Deep-Res. Pt. II*, 93, 16–32, <https://doi.org/10.1016/j.dsr2.2013.01.008>, 2013.
- López-Sandoval, D. C., Fernández, A., and Marañón, E.: Dissolved and particulate primary production along a longitudinal gradient in the Mediterranean Sea, *Biogeosciences*, 8, 815–825, <https://doi.org/10.5194/bg-8-815-2011>, 2011.
- Love, M. I., Huber, W., and Anders, S.: Moderated estimation of fold change and dispersion for RNA-seq data with DESeq2, *Genome Biol.*, 15, 1–21, <https://doi.org/10.1186/s13059-014-0550-8>, 2014.
- Ludwig, W., Dumont, E., Meybeck, M., and Heussner, S.: River discharges of water and nutrients to the Mediterranean and Black Sea: Major drivers for ecosystem changes during past and future decades?, *Prog. Oceanogr.*, 80, 199–217, <https://doi.org/10.1016/j.pocean.2009.02.001>, 2009.
- Luna, G. M., Bianchelli, S., Decembrini, F., De Domenico, E., Danovaro, R., and Dell'Anno, A.: The dark portion of the Mediterranean Sea is a bioreactor of organic matter cycling, *Global Biogeochem. Cy.*, 26, 1–14, <https://doi.org/10.1029/2011GB004168>, 2012.
- Mackas, D. L., Tsurumi, M., Galbraith, M. D., and Yelland, D. R.: Zooplankton distribution and dynamics in a North Pacific Eddy of coastal origin: II. Mechanisms of eddy colonization by and retention of offshore species, *Deep-Res. Pt. II*, 52, 1011–1035, <https://doi.org/10.1016/j.dsr2.2005.02.008>, 2005.
- Marañón, E., Cermeno, P., and Pérez, V.: Continuity in the photosynthetic production of dissolved organic carbon from eutrophic to oligotrophic waters, *Mar. Ecol. Prog. Ser.*, 299, 7–17, <https://doi.org/10.3354/meps299007>, 2005.
- Marañón, E., Van Wambeke, F., Uitz, J., Boss, E. S., Dimier, C., Dinasquet, J., Engel, A., Haëntjens, N., Pérez-Lorenzo, M., Taillandier, V., and Zäncker, B.: Deep maxima of phytoplankton biomass, primary production and bacterial production in the Mediterranean Sea, *Biogeosciences*, 18, 1749–1767, <https://doi.org/10.5194/bg-18-1749-2021>, 2021.
- Matis, P. A., Figueira, W. F., Suthers, I. M., Humphries, J., Miskiewicz, A., Coleman, R. A., Kelaher, B. P., and Taylor, M. D.: Cyclonic entrainment? The ichthyoplankton attributes of three major water mass types generated by the separation of the East Australian Current, *ICES J. Mar. Sci.*, 71, 1696–1705, <https://doi.org/10.1093/icesjms/fsu062>, 2014.
- Mazzocchi, M. G., Christou, E. D., Fragopoulou, N., and Siokoufrangou, I.: Mesozooplankton distribution from Sicily to Cyprus (Eastern Mediterranean): I. General aspects, *Oceanol. Acta*, 20, 521–535, 1997.
- McManus, G. B., Liu, W., Cole, R. A., Biemesderfer, D., and Mydosh, J. L.: *Strombidium rassoulzadegani*: A model species for chloroplast retention in Oligotrich Ciliates, *Front. Mar. Sci.*, 5, 1–11, <https://doi.org/10.3389/fmars.2018.00205>, 2018.
- McMurdie, P. J. and Holmes, S.: Phyloseq: An R Package for Reproducible Interactive Analysis and Graphics of Microbiome Census Data, *PLoS One*, 8, e61217, <https://doi.org/10.1371/journal.pone.0061217>, 2013.
- Menna, M., Poulain, P.-M., Zodiatis, G., and Gertman, I.: On the surface circulation of the Levantine sub-basin derived from Lagrangian drifters and satellite altimetry data, *Deep-Res. Pt. I*, 65, 46–58, <https://doi.org/10.1016/j.dsr.2012.02.008>, 2012.
- Mével, G., Vernet, M., Goutx, M., and Ghiglione, J. F.: Seasonal to hour variation scales in abundance and production of total and particle-attached bacteria in the open NW Mediterranean Sea (0–1000 m), *Biogeosciences*, 5, 1573–1586, <https://doi.org/10.5194/bg-5-1573-2008>, 2008.
- Miller, I., Sweatman, H., Cheal, A., Emslie, M., Johns, K., Jonker, M., and Osborne, K.: Origins and implications of a primary crown-of-thorns starfish outbreak in the southern great barrier reef, *J. Mar. Biol.*, 2015, 1–10, <https://doi.org/10.1155/2015/809624>, 2015.
- Mkhinini, N., Santi Coimbra, A. L., Stegner, A., Arsouze, T., Taupier-Letage, I., and Beranger, K.: Long-lived mesoscale eddies in the eastern Mediterranean Sea: Analysis of 20 years of AVISO geostrophic velocities, *J. Geophys. Res.-Oceans*, 119, 8603–8626, <https://doi.org/10.1002/2014JC010176>, 2014.
- Moore, C. M., Mills, M. M., Arrigo, K. R., Berman-Frank, I., Bopp, L., Boyd, P. W., Galbraith, E. D., Geider, R. J., Guieu, C., Jaccard, S. L., Jickells, T. D., La Roche, J., Lenton, T. M., Mahowald, N. M., Maranon, E., Marinov, I., Moore, J. K., Nakatsuka, T., Oschlies, A., Saito, M. A., Thingstad, T. F., Tsuda, A., and Ulloa, O.: Processes and patterns of oceanic nutrient limitation, *Nat. Geosci.*, 6, 701–710, <https://doi.org/10.1038/ngeo1765>, 2013.
- Motoda, S.: Devices of simple plankton apparatus, *Mem. Fac. Fish. Hokkaido University*, 7, 73–94, 1959.
- Mullaney, T. J. and Suthers, I. M.: Entrainment and retention of the coastal larval fish assemblage by a short-lived, submesoscale, frontal eddy of the East Australian Current, *Limnol. Oceanogr.*, 58, 1546–1556, <https://doi.org/10.4319/lo.2013.58.5.1546>, 2013.
- Nival, P., Nival, S., and Thiriou, A.: Influence des conditions hivernales sur les productions phyto- et zooplanctoniques en Méditerranée Nord-Occidentale. V. Biomasse et production zooplanctonique – relations phyto-zooplankton, *Mar. Biol.*, 31, 249–270, <https://doi.org/10.1007/BF00387153>, 1975.
- Olli, K., Wassmann, P., Reigstad, M., Ratkova, T. N., Arashkevich, E., Pasternak, A., Matrai, P. A., Knulst, J., Tranvik, L., Klais, R., and Jacobsen, A.: The fate of production in the central Arctic Ocean – top-down regulation by zooplankton expatriates?, *Prog. Oceanogr.*, 72, 84–113, <https://doi.org/10.1016/j.pocean.2006.08.002>, 2007.
- Ozer, T., Gertman, I., Kress, N., Silverman, J., and Herut, B.: Interannual thermohaline (1979–2014) and nutrient (2002–2014) dynamics in the Levantine surface and intermediate water masses, SE Mediterranean Sea, *Global Planet. Change*, 151, 60–67, <https://doi.org/10.1016/j.gloplacha.2016.04.001>, 2017.
- Palomera, I., Olivar, M. P., Salat, J., Sabatés, A., Coll, M., García, A., and Morales-Nin, B.: Small pelagic fish in the NW Mediterranean Sea: An ecological review, *Prog. Oceanogr.*, 74, 377–396, <https://doi.org/10.1016/j.pocean.2007.04.012>, 2007.
- Pancucci-Papadopoulou, M.-A., Siokou-Frangou, L., Theocharis, A., and Georgopoulos, D.: Zooplankton vertical distribution in relation to the hydrology in the NW Levantine, *Oceanol. Acta*, 15, 365–381, 1992.
- Parada, A. E., Needham, D. M., and Fuhrman, J. A.: Every base matters: Assessing small subunit rRNA primers for marine microbiomes with mock communities, time series and global field samples, *Environ. Microb.*, 18, 1403–1414, <https://doi.org/10.1111/1462-2920.13023>, 2016.
- Pasternak, A., Wassmann, P., and Riser, C. W.: Does mesozooplankton respond to episodic P inputs in the East-

- ern Mediterranean?, *Deep-Res. Pt. II*, 52, 2975–2989, <https://doi.org/10.1016/j.dsr2.2005.09.002>, 2005.
- Pinca, S. and Dallot, S.: Meso- and macrozooplankton composition patterns related to hydrodynamic structures in the Ligurian Sea (Trophos-2 experiment, April–June 1986), *Mar. Ecol. Prog. Ser.*, 126, 49–65, <https://doi.org/10.3354/meps126049>, 1995.
- Pinca, S. and Dallot, S.: Zooplankton community structure in the Western Mediterranean sea related to mesoscale hydrodynamics, *Hydrobiologia*, 356, 127–142, <https://doi.org/10.1023/a:1003151609682>, 1997.
- Pitta, P., Giannakourou, A., and Christaki, U.: Planktonic ciliates in the oligotrophic Mediterranean Sea: Longitudinal trends of standing stocks, distributions and analysis of food vacuole contents, *Aquat. Microb. Ecol.*, 24, 297–311, <https://doi.org/10.3354/ame024297>, 2001.
- Pitta, P., Nejtgaard, J. C., Tsagaraki, T. M., Zervoudaki, S., Egge, J. K., Frangoulis, C., Lagaria, A., Magiopoulos, I., Psarra, S., Sandaa, R.-A., Skjoldal, E. F., Tanaka, T., Thyrrhaug, R., and Thingstad, T. F.: Confirming the “Rapid phosphorus transfer from microorganisms to mesozooplankton in the Eastern Mediterranean Sea” scenario through a mesocosm experiment, *J. Plankton Res.*, 38, 502–521, <https://doi.org/10.1093/plankt/fbw010>, 2016.
- Pitta, P., Kanakidou, M., Mihalopoulos, N., Christodoulaki, S., Dimitriou, P. D., Frangoulis, C., Giannakourou, A., Kagiorgi, M., Lagaria, A., Nikolaou, P., Papageorgiou, N., Psarra, S., Santi, I., Tsapakis, M., Tsiola, A., Violaki, K., and Petihakis, G.: Saharan dust deposition effects on the microbial food web in the Eastern Mediterranean: A study based on a mesocosm experiment, *Front. Mar. Sci.*, 4, 1–19, <https://doi.org/10.3389/fmars.2017.00117>, 2017.
- Psarra, S., Tselepidis, A., and Ignatiades, L.: Primary productivity in the oligotrophic Cretan Sea (NE Mediterranean): seasonal and interannual variability, *Prog. Oceanogr.*, 46, 187–204, 2000.
- Pujo-Pay, M., Conan, P., Oriol, L., Cornet-Barthaux, V., Falco, C., Ghiglione, J.-F., Goyet, C., Moutin, T., and Prieur, L.: Integrated survey of elemental stoichiometry (C, N, P) from the western to eastern Mediterranean Sea, *Biogeosciences*, 8, 883–899, <https://doi.org/10.5194/bg-8-883-2011>, 2011.
- Pulido-Villena, E., Ghiglione, J. F., Ortega-Retuerta, E., Van-Wambeke, F., and Zohary, T.: Heterotrophic bacteria in the pelagic realm of the Mediterranean Sea, in: *Life in the Mediterranean Sea: A Look at Habitat Changes*, edited by: Stambler, N., pp. 227–265, Nova Science Publishers, NY, 2012.
- R Core Team: R: A Language and Environment for Statistical Computing, Vienna, Austria, <https://www.R-project.org/> (last access: May 2022), 2018.
- Rabi, C., Rilov, G., Morov, A. R., and Guy-Haim, T.: First record of the red sea gastropod *nerita sanguinolenta menke*, 1829 (Gastropoda: Cycloneritida: Neritidae) from the israeli mediterranean coast, *BioInvasions Rec.*, 9, 496–503, <https://doi.org/10.3391/bir.2020.9.3.06>, 2020.
- Rahav, E., Herut, B., Stambler, N., Bar-Zeev, E., Mulholland, M. R., and Berman-Frank, I.: Uncoupling between dinitrogen fixation and primary productivity in the eastern Mediterranean Sea, *J. Geophys. Res.-Biogeo.*, 118, 195–202, <https://doi.org/10.1002/jgrg.20023>, 2013.
- Rahav, E., Silverman, J., Raveh, O., Hazan, O., Rubin-Blum, M., Zeri, C., Gogou, A., Kralj, M., Pavlidou, A., and Kress, N.: The deep water of Eastern Mediterranean Sea is a hotspot for bacterial activity, *Deep-Res. Pt. II*, 164, 135–143, <https://doi.org/10.1016/j.dsr2.2019.03.004>, 2019.
- Rahav, E., Herut, B., Spungin, D., Levi, A., Mulholland, M. R., and Berman-Frank, I.: Heterotrophic bacteria outcompete diazotrophs for orthophosphate in the Mediterranean Sea, *Limnol. Oceanogr.*, 9999, 1–13, <https://doi.org/10.1002/lno.11983>, 2021.
- Rakshesh, M., Raman, A. V., Kalavati, C., Subramanian, B. R., Sharma, V. S., Sunitha Babu, E., and Sateesh, N.: Zooplankton community structure across an eddy-generated upwelling band close to a tropical bay-mangrove ecosystem, *Mar. Biol.*, 154, 953–972, <https://doi.org/10.1007/s00227-008-0991-2>, 2008.
- Reich, T., Ben-Ezra, T., Belkin, N., Tsemel, A., Aharonovich, D., Roth-rosenberg, D., Givati, S., Bialik, M., Herut, B., Berman-Frank, I., Frada, M., Krom, M. D., Lehahn, Y., Rahav, E., and Sher, D.: A year in the life of the Eastern Mediterranean: Monthly dynamics of phytoplankton and bacterioplankton in an ultra-oligotrophic sea, *Deep-Sea Res. Pt. I*, 182, 103720, <https://doi.org/10.1016/j.dsr.2022.103720>, 2022.
- Riandey, V., Champalbert, G., Carlotti, F., Taupier-Letage, I., and Thibault-Botha, D.: Zooplankton distribution related to the hydrodynamic features in the Algerian Basin (western Mediterranean Sea) in summer 1997, *Deep-Res. Pt. I Oceanogr. Res. Pap.*, 52, 2029–2048, <https://doi.org/10.1016/j.dsr.2005.06.004>, 2005.
- Ridame, C., Le Moal, M., Guieu, C., Ternon, E., Biegala, I. C., L’Helguen, S., and Pujo-Pay, M.: Nutrient control of N<sub>2</sub> fixation in the oligotrophic Mediterranean Sea and the impact of Saharan dust events, *Biogeosciences*, 8, 2773–2783, <https://doi.org/10.5194/bg-8-2773-2011>, 2011.
- Robinson, A. R. and Golnaraghi, M.: The physical and dynamical oceanography of the Eastern Mediterranean Sea, in: *Ocean Processes in Climate Dynamics: Global and Mediterranean Examples*, edited by: Malanotte-Rizzoli, P. and Robinson, A. R., pp. 255–306, Springer Netherlands, Dordrecht, 1994.
- Sala, M. M., Peters, F., Gasol, J. M., Pedrós-Alió, C., Marasé, C., and Vaqué, D.: Seasonal and spatial variations in the nutrient limitation of bacterioplankton growth in the northwestern Mediterranean, *Aquat. Microb. Ecol.*, 27, 47–56, <https://doi.org/10.3354/ame027047>, 2002.
- Santi, I., Kasapidis, P., Psarra, S., Assimakopoulou, G., Pavlidou, A., Protopapa, M., Tsiola, A., Zeri, C., and Pitta, P.: Composition and distribution patterns of eukaryotic microbial plankton in the ultra-oligotrophic Eastern Mediterranean Sea, *Aquat. Microb. Ecol.*, 84, 155–173, 2020.
- Sathyendranath, S. and Platt, T.: Spectral effects in bio-optical control on the ocean system, *Oceanologia*, 49, 5–39, 2007.
- Seguin, G., Errhif, A., and Dallot, S.: Diversity and structure of pelagic copepod populations in the frontal zone of the eastern Alboran sea, *Hydrobiologia*, 292–293, 369–377, <https://doi.org/10.1007/BF00229962>, 1994.
- Sherr, E. B. and Sherr, B. F.: Heterotrophic dinoflagellates: A significant component of microzooplankton biomass and major grazers of diatoms in the sea, *Mar. Ecol. Prog. Ser.*, 352, 187–197, <https://doi.org/10.3354/meps07161>, 2007.
- Simon, M., Alldredge, A., and Azam, F.: Protein-content and protein-synthesis rates of planktonic marine-bacteria, *Mar. Ecol. Prog. Ser.*, 51, 201–213, 1989.

- Siokou-Frangou, I.: Epipelagic mesozooplankton and copepod grazing along an east–west transect in the Mediterranean Sea, *Mar. Biol.*, 144, 1111–1126, 2004.
- Siokou-Frangou, I., Christou, E. D., Gotsis-Scretas, O., Kontoyianis, H., Krasakopoulou, E., Pagou, K., Pavlidou, A., Souvermezoglou, E., and Theocharis, A.: Impact of physical processes upon chemical and biological properties in the Rhodes gyre area, in: *International Conference: Progress in Oceanography of the Mediterranean Sea*, Rome, November, pp. 17–19., 1997.
- Siokou-Frangou, I., Bianchi, M., Christaki, U., Christou, E. D., Giannakourou, A., Gotsis, O., Ignatiades, L., Pagou, K., Pitta, P., Psarra, S., Souvermezoglou, E., Van Wambeke, F., and Zervakis, V.: Carbon flow in the planktonic food web along a gradient of oligotrophy in the Aegean Sea (Mediterranean Sea), *J. Marine Syst.*, 33–34, 335–353, [https://doi.org/10.1016/S0924-7963\(02\)00065-9](https://doi.org/10.1016/S0924-7963(02)00065-9), 2002.
- Siokou-Frangou, I., Christaki, U., Mazzocchi, M. G., Montresor, M., Ribera d’Alcalá, M., Vaqué, D., and Zingone, A.: Plankton in the open Mediterranean Sea: a review, *Biogeosciences*, 7, 1543–1586, <https://doi.org/10.5194/bg-7-1543-2010>, 2010.
- Sisma-Ventura, G. and Rahav, E.: DOP Stimulates Heterotrophic Bacterial Production in the Oligotrophic Southeastern Mediterranean Coastal Waters, *Front. Microbiol.*, 10, 1913, <https://doi.org/10.3389/fmicb.2019.01913>, 2019.
- Smith, D. C., Smith, D. C., Azam, F., and Azam, F.: A simple, economical method for measuring bacterial protein synthesis rates in seawater using <sup>3</sup>H-leucine, *Marine Microbial Food Webs*, 6, 107–114, 1992.
- Stambler, N.: Underwater light field of the Mediterranean Sea, in: *Life in the Mediterranean Sea: A Look at Habitat Changes*, edited by: Stambler, N., Nova Science Publishers, NY, 175–198, ISBN 978-1-61209-644-5, 2012.
- Steemann-Nielsen, E.: The use of radioactive carbon (<sup>14</sup>C) for measuring organic production in the sea, *Journal of the International Council for the Exploration of the Sea.*, 18, 117–140, 1952.
- Stergiou, K. I., Christou, E. D., and Petrakis, G.: Modelling and forecasting monthly fisheries catches: Comparison of regression, univariate and multivariate time series methods, *Fish. Res.*, 29, 55–95, [https://doi.org/10.1016/S0165-7836\(96\)00482-1](https://doi.org/10.1016/S0165-7836(96)00482-1), 1997.
- Strzelecki, J., Koslow, J. A., and Waite, A.: Comparison of mesozooplankton communities from a pair of warm- and cold-core eddies off the coast of Western Australia, *Deep-Res. Pt. II*, 54, 1103–1112, <https://doi.org/10.1016/j.dsr2.2007.02.004>, 2007.
- Suzuki, N., Ogane, K., Aita, Y., Kato, M., Sakai, S., Kurihara, T., Matsuoka, A., Ohtsuka, S., Go, A., Nakaguchi, K., Yamaguchi, S., Takahashi, T., and Tuji, A.: Distribution patterns of the radiolarian nuclei and symbionts using DAPI-fluorescence, *Bull. Natl. Mus. Nat. Sci. Ser. B*, 35, 169–182, 2009.
- Tanaka, T., Thingstad, T. F., Christaki, U., Colombet, J., Cornet-Barthaux, V., Courties, C., Grattapanche, J.-D., Lagaria, A., Nedoma, J., Oriol, L., Psarra, S., Pujo-Pay, M., and Van Wambeke, F.: Lack of P-limitation of phytoplankton and heterotrophic prokaryotes in surface waters of three anticyclonic eddies in the stratified Mediterranean Sea, *Biogeosciences*, 8, 525–538, <https://doi.org/10.5194/bg-8-525-2011>, 2011.
- Thingstad, T. F., Krom, M. D., Mantoura, R. F. C., Flaten, G. a F., Groom, S., Herut, B., Kress, N., Law, C. S., Pasternak, a, Pitta, P., Psarra, S., Rassoulzadegan, F., Tanaka, T., Tselepidis, A., Wassmann, P., Woodward, E. M. S., Riser, C. W., Zodiatis, G., and Zohary, T.: Nature of phosphorus limitation in the ultraoligotrophic eastern Mediterranean, *Science*, 309, 1068–71, <https://doi.org/10.1126/science.1112632>, 2005.
- Tsiola, A., Tsagaraki, T. M., Giannakourou, A., Nikolioudakis, N., Yücel, N., Herut, B., and Pitta, P.: Bacterial growth and mortality after deposition of Saharan dust and mixed aerosols in the Eastern Mediterranean Sea: a mesocosm experiment, *Front. Mar. Sci.*, 3, 1–13, <https://doi.org/10.3389/fmars.2016.00281>, 2017.
- Vaillancourt, R. D., Marra, J., Seki, M. P., Parsons, M. L., and Bidigare, R. R.: Impact of a cyclonic eddy on phytoplankton community structure and photosynthetic competency in the subtropical North Pacific Ocean, *Deep-Res. Pt. I*, 50, 829–847, [https://doi.org/10.1016/S0967-0637\(03\)00059-1](https://doi.org/10.1016/S0967-0637(03)00059-1), 2003.
- Van-Ruth, P., Redondo Rodriguez, A., Davies, C., and Richardson, A. J.: Indicators of depth layers important to phytoplankton production, *Deep-Sea Res. Pt. II*, 157–158, 36–45, 2020.
- Van Wambeke, F., Christaki, U., Giannakourou, A., Moutin, T., Souvermezoglou, E., and Giannokourou, A.: Longitudinal and vertical trends of bacterial limitation by phosphorus and carbon in the Mediterranean Sea, *Microb. Ecol.*, 43, 119–133, 2002.
- Waite, A. M., Thompson, P. A., Pesant, S., Feng, M., Beckley, L. E., Domingues, C. M., Gaughan, D., Hanson, C. E., Holl, C. M., Koslow, T., Meuleners, M., Montoya, J. P., Moore, T., Muhling, B. A., Paterson, H., Rennie, S., Strzelecki, J., and Twomey, L.: The Leeuwin Current and its eddies: An introductory overview, *Deep-Res. Pt. II*, 54, 789–796, <https://doi.org/10.1016/j.dsr2.2006.12.008>, 2007.
- Welschmeyer, N. A.: Fluorometric analysis of chlorophyll a in the presence of chlorophyll b and pheopigments, *Limnol. Oceanogr.*, 39, 1985–1992, 1994.
- Wickham, H.: Ggplot2, *WIREs Comput. Stat.*, 3, 180–185, <https://doi.org/10.1002/wics.147>, 2011.
- Zhou, M., Carlotti, F., and Zhu, Y.: A size-spectrum zooplankton closure model for ecosystem modelling, *J. Plankton Res.*, 32, 1147–1165, <https://doi.org/10.1093/plankt/fbq054>, 2010.
- Zohary, T. and Robarts, R. R. D.: Experimental study of microbial P limitation in the eastern Mediterranean, *Limnol. Oceanogr.*, 43, 387–395, <https://doi.org/10.4319/lo.1998.43.3.0387>, 1998.
- Zohary, T., Herut, B., Krom, M. D., Fauzi C. Mantoura, R., Pitta, P., Psarra, S., Rassoulzadegan, F., Stambler, N., Tanaka, T., Frede Thingstad, T., and Malcolm S. Woodward, E.: P-limited bacteria but N and P co-limited phytoplankton in the Eastern Mediterranean – A microcosm experiment, *Deep-Res. Pt. II*, 52, 3011–3023, <https://doi.org/10.1016/j.dsr2.2005.08.011>, 2005.